Research in Pharmaceutical Sciences, August 2025; 20(4): 535-565
Received: 19-7-2024
Peer Reviewed: 24-08-2024
Revised: 08-11-2024
Accepted: 10-11-2024
Published: 25-08-2025

School of Pharmacy & Pharmaceutical Sciences
Isfahan University of Medical Sciences

Original Article

Molecular docking and simulation analysis of selected herbal compounds against GP63, FPPS, and NMT, three important *Leishmania major* proteins

Seyed Mahmoud Mousavi[1], Negar Balmeh[2], Najaf Allahyari Fard[3], Zahra Ghayour Najafabadi[1], Sedighe Saberi[1], Hajar Shabandoust[1], Parisa Mousavi[4], Shima Gharibi[5], Mustafa Ghanadian[6,*], and Seyed Hossein Hejazi[1,4,*]

[1]*Department of Parasitology and Mycology, School of Medicine, Isfahan University of Medical Sciences, Isfahan, Iran.*
[2]*Department of Research and Development, Darou Giah Pars Avid Company, Science and Research Town, Isfahan, Iran.*
[3]*Systems Biotechnology Department, National Institute of Genetic Engineering and Biotechnology (NIGEB),Tehran, Iran.*
[4]*Skin Diseases and Leishmaniasis Research Center, Isfahan University of Medical Sciences, Isfahan, Iran.*
[5]*Core Research Facilities (CRF), Isfahan University of Medical Sciences, Isfahan, Iran.*
[6]*Department of Pharmacognosy and Isfahan Pharmaceutical Sciences Research Center, School of Pharmacy and Pharmaceutical Sciences, Isfahan University of Medical Sciences, Isfahan, Iran.*

Abstract

Background and purpose: Leishmaniasis has been categorized as one of the most significant tropical illnesses, often ignored. This study aimed to find effective plant compounds to combat the pathogenicity of the *Leishmania* parasite.
Experimental approach: The 3D structures of the zinc leishmanolysin glycoprotein 63 (GP63), farnesyl diphosphate synthase (FPPS), and N-myristoyltransferase (NMT) proteins from *L. major*, as well as blockers and 4000 herbal compounds, were retrieved from the PubChem database. A molecular docking study was performed on *Leishmania* proteins using PyRx software. The activity, ADMET characteristics, and daily carcinogenicity were taken from "Swiss ADME", "way 2 drug", and "Lazar" websites. Molecules with the greatest docking scores for each protein were chosen for molecular dynamics simulation using GROMACS.
Findings/Results: Molecular docking experiments revealed that withaperuvin D and lagerstannin A have a strong affinity for the GP63 protein. Moreover, strictinin showed the highest binding affinity for FPPS, whereas the top compounds for NMT were chelidimerine, friedelin, and hypericin. Additionally, luteolin 3'-o-glucuronide, protohypericin, and amentoflavone had high binding affinity for all three proteins, and amentoflavone had the highest binding energy of all the proteins. Based on RMSD, RMSF, Rg, PCA, MM/PBSA binding energy, and SASA, the molecular dynamic simulation results indicated relatively stable interactions between these ligands and the mentioned proteins during the simulation period.
Conclusion and implications: Given the pharmaceutical information, the mentioned substances may have anti-inflammatory and wound-healing properties in addition to blocking proteins. Therefore, experimentally examining these compounds in the future can help control and treat leishmaniasis.

Keywords: FPPS; GP63; Herbal compounds; Leishmaniasis; Molecular dynamics; NMT.

INTRODUCTION

The protozoan parasite *Leishmania*, which causes a spectrum of diseases known as leishmaniasis, is spread by female mosquitoes Phlebotomus (old world) and Lutzomia (new world) as its vectors. There are two different forms of *Leishmania*: amastigote and promastigote.

*Corresponding authors:
S.H. Hejazi, Tel: +98-9133118711, Fax: +98-3137929170
Email: hejazi@med.mui.ac.ir
M. Ghanadian, Tel: +98-9133167326, Fax: +98-3133344798
Email: ghannadian@pharm.mui.ac.ir

Access this article online
Website: http://rps.mui.ac.ir
DOI: 10.4103/RPS.RPS_123_24

Amastigotes are intracellular, spherical, non-flagellated cells that do not possess motility. They proliferate within the phagolysosomes of the macrophages of the vertebrate host (1,2). The treatment of leishmaniasis is significant since it can have unsafe side effects and cause lethal results (3).

Leishmania contains a few proteins that can be successfully targeted for the inhibition of leishmaniasis. Although glycoprotein 63 (GP63) is the most prominent surface protein in promastigotes and constitutes 1% of the total parasite proteome, GP63 expression also increases in amastigotes.

According to certain reports, GP63 interatomic with the fibronectin proteins, which may offer assistance to the parasite, and adheres to macrophages even more. From these changes that have come about, GP63 can altogether modify the activities of macrophages, by changing a few key signaling pathways, for instance, JAK, MAP, and outline favoring *Leishmania* survival (Fig. 1) (4). The glycol protein GP63 plays a part in the resistance of promastigotes against antagonistic conditions, complement-mediated lysis, as well as the take-up of *Leishmania* by protein receptors. The hindrance of GP63, a potential restorative target and immunization candidate, ruins the connection of promastigote shape to the macrophage and its change into the amastigote state inside the macrophage, thus smothering *Leishmania* (5).

Farnesyl diphosphate synthase (FPPS), an enzyme of the isoprenoid biosynthesis pathway responsible for the synthesis of vital isoprenoids, such as carotenoids, chlorophylls, ubiquinones, dolichols, and sterols, is the next significant protein in *Leishmania* regulation and one of the therapeutic targets. FPPS is a crucial mediator of sterol metabolism that participates in the farnesyltransferase-mediated post-translational modification of proteins, as well as prenylation of Ras, Rho, Rac, and Rab family proteins, crucial GTPase factors (Fig. 2) (6). Therefore, FPPS have a special relationship with *L. major* due to their importance for parasite survival as a possible target for the development of antiparasitic drugs against *Trypanosoma brucei*, *T. cruzi*, *L. donovani*, *Toxoplasma gondii*, and *Plasmodium falciparum* (7). Since most *Leishmania* strains share more than 90% of the FPPS sequence, it might be possible to create drugs that inhibit this enzyme universally (8).

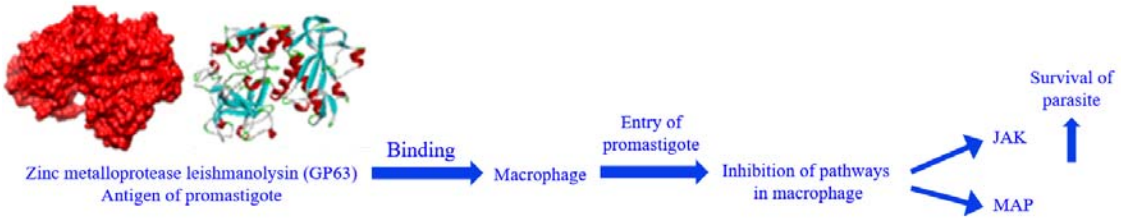

Fig. 1. GP63 mechanism of action in *Leishmania major*. GP63, Glycoprotein 63.

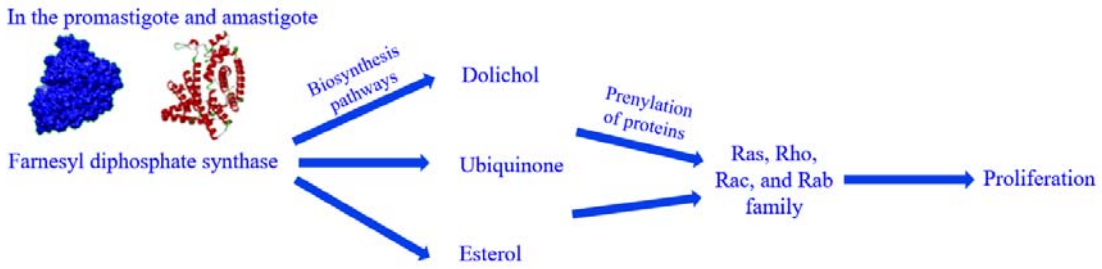

Fig. 2. Farnesyl diphosphate synthase mechanism of action in *Leishmania major*.

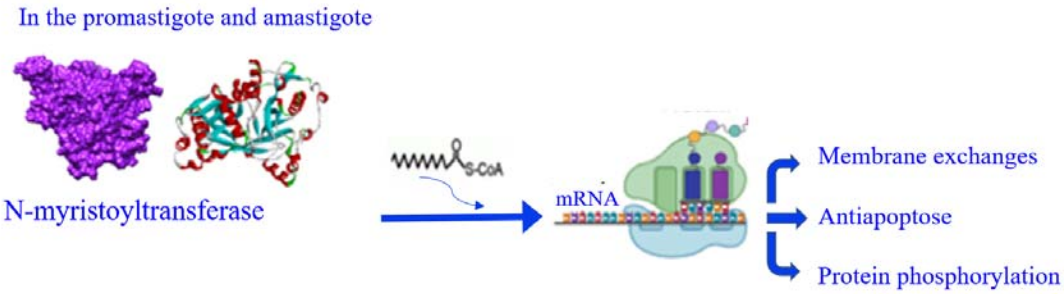

Fig. 3. N-myristoyltransferase mechanism of action in *Leishmania major*.

Another significant *Leishmania* protein is N-myristoyltransferase (NMT), which has been shown in earlier studies to be a viable candidate for the synthesis of medications against dangerous protozoan parasites (9, 10). NMT catalyzes the attachment of 14-carbon saturated fatty acid, myristate, to the amino-terminal glycine residue of a subset of eukaryotic proteins that function in numerous cellular processes, including vesicular protein trafficking and signal transduction. In addition to facilitating protein-protein interactions, this modification helps target substrate proteins to membrane regions (11). In general, N-myristoylated proteins are likely to be preserved with vital capacities, including transport, protein phosphorylation, proteasomal degradation, and Golgi function, in both life stages of *Leishmania* (Fig. 3) (12). These factors indicated that NMT is a suitable candidate for the treatment of infectious diseases and parasites, including malaria (caused by *Plasmodium spp.*), leishmaniasis (caused by *Leishmania spp.*), and African sleeping sickness (caused by *Trypanosoma brucei*). *Leishmania* NMT inhibitors have recently been developed and demonstrated to inhibit the development of critical intracellular structures and cause rapid death of parasite cells, as this protein is necessary for the survival of promastigotes in the insect stage, as confirmed genetically by targeted gene disruption techniques (13,14).

Since the drug resistance of this parasite has increased a lot, and in most cases, this resistance causes the treatment to fail, and considering the side effects of existing drugs, it is very important to design and discover new drugs to treat this disease. These three proteins are essential for the parasite's survival and virulence, and they can be inhibited to kill the parasite. Meglumine antimoniate (glucantime), sodium stibogluconate (pentostam), and pentamidine (pentacarinate), which are the first-line treatments for leishmaniasis, have toxicity and side effects that make them ineffective when taken orally and necessitate long-term injections (15, 16). Second-line medications include very toxic amphotericin B and pentamidine, as well as the teratogenic miltefosine (Miltex), an alkylphospholipid used in cancer treatment. Scientists are continuously searching the globe for novel countermeasures to combat multidrug resistance (17,18). Numerous studies have shown that different plant species have inhibitory activity against most parasites. Leishmaniasis can be treated with various plant oils because they have regulatory effects on the immune system. In this context, various plant extracts with leishmanicidal activity are suggested for use, including alkaloids, chalcones, phenolics, and terpenes (19). Thus, clinical trials for immunization strategies have not yet begun. Therefore, it is urgently necessary to create new, more potent medications with enhanced qualities to either replace or supplement those already on the market. It is anticipated that efficient medications made from plant derivatives or extracts would become an important resource. Less than 1% of herbal medicinal substances were tested in clinical studies to treat leishmaniasis (20-23). Bioinformatic studies are very advantageous, particularly in the realm of drug development, due to the time-consuming and costly nature of laboratory research, as well as the inherent risks associated with dealing with pathogenic microorganisms. Also, in order to answer particular questions concerning the structural characteristics and dynamical mechanisms of

model systems, molecular dynamics (MD) simulation is frequently used in physics, chemistry, and biology. It permits one to forecast the time evolution of a system of interacting particles.

So, a bioinformatic approach was conducted to inhibit three important proteins of the *L. major* parasite. The active substances from plants were docked against the NMT, GP63, and FPPS proteins of *L. major* to find the best compounds for inhibiting them. In addition, an MD simulation study was conducted to assess the stability of the chosen compounds. Subsequently, the pharmacological characteristics of the compounds with the most favorable outcomes were examined to identify potential targets for experimental investigations. However, the efficacy of these compounds needs to be experimentally confirmed (Fig. 4).

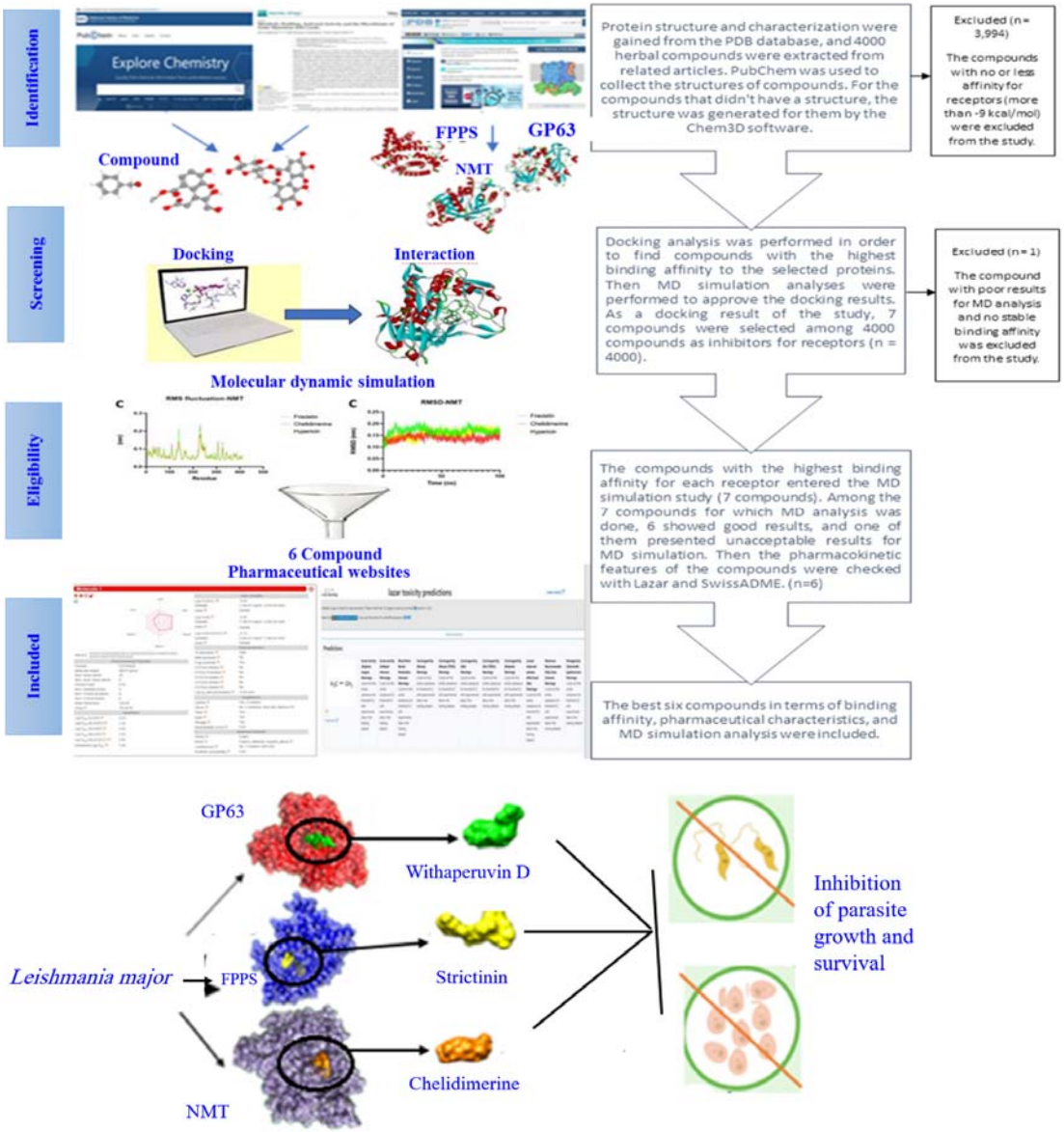

Fig. 4. Systematic review flow diagram. The PRISMA flow diagram for the study. GP63, Glycoprotein 63; FPPS, farnesyl diphosphate synthase; NMT, N-myristoyltransferase.

MATERIALS AND METHODS

Finding protein structure and characterization

L. major proteins' structure, ligand binding sites, and PDB ID were obtained from previous articles. Table 1 depicts important target proteins of *L. major*, GP63, FPPS, NMT, PDB ID, and important amino acids involved in interaction with inhibitors. Protein PDB structure was gained from the RCSB PDB database (https://www.rcsb.org) (24).

Collecting the herbal phytochemicals

First, we collected the names of most of the Iranian medicinal plants, then, according to the articles that specified the active ingredients of each, we obtained 300 plants and 4000 active ingredients from different plant parts, and collected their 3D structure from the Pubchem database. (22,23,32-35). The studies that used validating methods for phytochemical screening, including GC/MS and HPLC, were used to extract 4000 compounds (36-38). The compounds of each plant were examined in all available articles. The names of the desired plants are presented in Table S1. 3D structure of 4000 compounds from 300 herbs, and that of each protein's probable blockers were obtained from the PubChem database (https://pubchem.ncbi.nlm.nih.gov/) (39), and those that did not have a structure were modeled by Chem3D software version 21.0.0.

Preparation and molecular docking analysis

3D structures of protein blockers and herbal compounds were prepared for docking by removing all water and H-bond optimization, and then, Gasteiger charges were added. Proteins and ligands were changed over to PDBQT organize (a organize that incorporates charges and types of particles), and at long last, a space was chosen for the dock that contains all the amino acids specified in Table 1 and agreed to the dynamic location of the protein. The location facilitates intuitive (network estimate) utilized for GP63 are center: 20.2471, 40.6108, and 18.2018, and estimate:16.7421, 20.6414, and 19.9465, for FPPS center: 16.9245, 41.478, and 125.318, and estimate: 20.9211, 29.8813, and 25.1407, and NMT center: 4.63281, 49.5063, and 62.6636, and estimate: 25.3756, 23.6199, and 25.1636. Then, molecular docking analysis was performed for each of the three *Leishmania* proteins separately with herbal compounds and protein blockers using PyRx software version 0.8, and then those with a score of -8 kcal/mol or less were docked with the corresponding protein by AutoDock vina chimera software version 1.16. Figures of proteins and compounds were made by Chimera software version 1.14. (40), and Discovery Studio 2021 (41).

Analysis of complex interactions

The compounds with the highest Dock score were selected for each of the target proteins, and subsequently, their interactions were thoroughly examined. In addition, articles related to the treatment of Leishmania were considered. Among the numerous proposed blockers, those with the highest docking scores were selected for re-docking using AutoDock Vina, and their interactions with three *Leishmania* proteins were analyzed in detail.

Determination of pharmacokinetic features of compounds with a high docking score

The activity, carcinogenicity, and absorption, distribution, metabolism, excretion, and toxicity (ADMET) features of compounds with high scores caught from the Way 2 Drug website (42) (www.pharmaexpert.ru/passonline/predict.php), Lazar (43) (lazar.in-silico.ch/predict), and a free and accessible SwissADME website (44) (http://www.swissadme.ch), respectively.

MD simulation analysis

After docking, compounds with the highest score for each protein were selected for MD simulation analysis. The structures obtained from the docking simulation were refined using an MD simulation. Structural refinement was conducted using GROningen MAchine for Chemical Simulations GROMACS 4.6.5. The stability of the complex structure was assessed by performing MD simulations using GROMACS version 5 for all complexes (http://gromacs.org) (45).

Table 1. PDB ID and important amino acids involved in the interaction of GP63, FPPS, and NMT proteins with plant compounds.

Protein name	Code PDB	Resolution	Amine acids	Reference No.
GP63	1LML	1.86 Å	HIS264, HIS268, HIS334, MET345, ALA348, ALA227, SER273, GLY222, THR228, GLU265, ALA350, PRO347, VAL223, GLY329, GLU220	(25)
			LEU224, ALA225, SER418, GLN341, GLY222, SER465, VAL223, HIS264, LEU257, PRO460, ALA350	(26)
			HIS264, ASP342, HIS268, HIS334, MET345, ALA348, PHE272, SER333	(17)
FPPS	4K10	2.30 Å	LYS207, LYS264, ARG107, ASP102, ASP98, ASP99, ASP250, PHE94, LEU95, HIS93, MET101, GLN167	(27)
			ARG107, GLN167, LYS264, ASP268, THR267, ASP170, LYS207	(28)
			LYS207, LYS264, ARG107, PHE94, GLN167, THR163, ASP102, ASP98, ASP250, ASP254	(19) (29)
			ASP98, ILE100, MET101, ASP102, ARG107, ARG108, HIS93, PHE94	
NMT	4CGO	1.30 Å	PHE90, VAL81, PHE232, GLY397, PHE88, HIS219, ASP83, GLY205, TYR80, TYR217, LEU421, TYR345, LEU341, TYR92, ASN167, HIS398, ALA204, VAL374, ALA343, ASN376	(9)
			TYR92, PHE90, ASN167, PHE88, THR203, HIS219, TYR217, PHE232, TYR326, VAL81, TYR80, GLU82, ILE328, SER330, LEU341, MET420, LEU421, ASP396, LEU399, ASP396, ASN376, VAL374, TYR345, ALA343	(30)
			ALA204, TYR202, PHE90, MET420, TYR326, TYR345, LEU421, ASN167, VAL81, ASN383, TYR80, VAL378, LYS173, GLU82	(31)

GP63, Glycoprotein 63; FPPS, farnesyl diphosphate synthase; NMT, N-myristoyltransferase.

The complex was then put through a simulation lasting 100000 ps to uncover its dynamic behavior and identify its pattern of interaction. The force fields utilized to neutralize the SPC model for filling the water with a pressure of 1 bar, at 300 K, and a neutral pH set were Gromos 54A7, sodium (Na^+), and chloride (Cl^-) ions. The systems were first brought into equilibrium under 100 ps NVT at 298 K, then under 100 ps NPT ensembles at 1 bar of pressure. PME was used to determine electrostatic interactions, and the LINCS technique was used to limit all bonds joining hydrogen atoms. Without any restraint, the final MD simulation was conducted for 100000 ps. The physical motions of atoms and molecules were then observed to produce the root-mean-square fluctuation (RMSF), root-mean-square deviation (RMSD), principal component analysis (PCA), solvent accessible surface area (SASA), molecular mechanics Poisson-Boltzmann surface area (MMPBSA), H-bound, and radius of gyration (RG) diagrams of the simulated complex protein. Using the GROMACS software, the compounds with the best docking scores for each protein were selected for MD simulation (46).

The binding energy calculated by the MM-PBSA method

Using the ΔGMMPBSA method, we were able to ascertain the binding free energy for each protein-ligand pairing during the MD simulations. Utilizing the MMPBSA method, the energy decomposition feature of gmx_MMPBSA was used to calculate the contribution of the residue (47). Free energy in the gas phase (ΔG_{gas}) and the free energy in the dissolved phase (ΔG_{Solv}) are added to create ΔGMMPBSA. The energy gained from adding the bonding and non-bonding energy is known as "ΔG_{gas}". Bond, angle, and dihedral energy make up the bonding energy, while van der Waals energy and electronic energy contribute to the non-bonding energy. In the ΔG_{MMPBSA} computation, Poisson-Boltzmann energy, non-polar solvation energy, and dispersion energy all contribute to ΔG_{Solv}. The other energies are non-polar, whereas the Poisson-Boltzmann energy is polar.

Supplementary materials

Table S1 is available at: https://github.com/mahmoud452124/Names-of-medicinal-plants.git

RESULTS

Docking analysis

The best herbal compounds for GP63, FPPS, and NMT proteins were identified based on their binding energy and the type of bonds and interactions. Molecular docking results are shown in Table 2. Withaperuvin D and lagerstannin A were the best compounds with the highest binding affinity for GP63 (Table 2 and Figs. 5 and 6). Strictinin was the best compound for interaction with FPPS (Table 2 and Fig. 7). Chelidimerine, friedelin, and hypericin were the compounds with the highest affinity for NMT (Table 2 and Figs. 8-10). After selecting the compounds with the highest binding energies, the selected substances were also checked in terms of the type and number of bonds.

The common compounds with a high affinity for each protein

Amentoflavone, protohypericin, and luteolin 3'-o-glucuronide were common among all three proteins. The docking score of each compound for each protein is shown in Table 3.

The interactions of proposed compounds with the amino acids of 3 important proteins of L. major

The intelligence of bisphosphonate compounds repressing GP63 protein in its dynamic location is as follows. Five hydrogen bonds with His235, Gly230, Ala126, Leu125, and Ala250 amino acids with separations of 3.485, 3.323, 2.657, 2.285, and 2.444 Å, respectively. It has electrostatic interactions with Glu166 and His165, with a docking score of -5.7 kcal/mol. Podocarpusflavone A has two hydrogen bonds with amino acids, Thr129 and Ala249, and two more hydrogen bonds with Ser234. The compound's six-membered rings engage in hydrophobic interactions with the His169 amino acid. Additionally, this molecule forms two Pi-Anion electrostatic contacts with the amino acid Glu166. The molecule has a binding energy of -8.5 kcal/mol. In the case of withaperuvin D, the formation of a suitable hydrogen bond between amino acids Ala225, Glu265, and His268 at the active site of GP63 protein requires the presence of different OH groups on the rings of this compound.

Table 2. Plant name, docking scores of each herbal active with GP63, FPPS, and NMT proteins.

Protein name	Compound	Molecular formula	IUPAC Name	Herb name	Docking score (kcal/mol)
GP63	Withaperuvin D	$C_{28}H_{40}O_9$	(1S,3R,4R,7S,8S,11S,12R,15R,16S,17R)-7-[(1S)-1-[(2R)-4,5-dimethyl-6-oxo-2,3-dihydropyran-2-yl]-1-hydroxyethyl]-4,7,16,17-tetrahydroxy-8,12-dimethyl-18-oxapentacyclo[13.2.1.$0^{3,11}$.$0^{4,8}$.$0^{12,17}$]octadecan-13-one	*Plantago psyllium*	-9.2
	Lagerstannin A	$C_{34}H_{24}O_{23}$	(10R,11S)-11-[(10R,11R)-3,4,5,11,17,18,19-heptahydroxy-8,14-dioxo-9,13-dioxatricyclo[13.4.0.$0^{2,7}$]nonadeca-1(19),2,4,6,15,17-hexaen-10-yl]-3,4,5,16,17,18-hexahydroxy-8,13-dioxo-9,12-dioxatricyclo[12.4.0.$0^{2,7}$]octadeca-1(18),2,4,6,14,16-hexaene-10-carboxylic acid	*Punica granatum*	-9.2
	Physagulin D	$C_{34}H_{52}O_{10}$	(2R)-2-[(1S)-1-[(1S,3R,8S,9S,10R,13S,14S,17R)-1-hydroxy-10,13-dimethyl-3-[(2R,3R,4S,5S,6R)-3,4,5-trihydroxy-6-(hydroxymethyl)oxan-2-yl]oxy-2,3,4,7,8,9,11,12,14,15,16,17-dodecahydro-1H-cyclopenta[a]phenanthren-17-yl]ethyl]-5-(hydroxymethyl)-4-methyl-2,3-dihydropyran-6-one	*Withania somnifera*	-9.1
	Luteolin 7-O-(6''-malonylglucoside)	$C_{24}H_{22}O_{14}$	3-[[(2R,3S,4S,5R,6S)-6-[2-(3,4-dihydroxyphenyl)-5-hydroxy-4-oxochromen-7-yl]oxy-3,4,5-trihydroxyoxan-2-yl]methoxy]-3-oxopropanoic acid	*Chrysanthemum morifolium*	-9.0
	Amentoflavone	$C_{30}H_{18}O_{10}$	8-[5-(5,7-dihydroxy-4-oxochromen-2-yl)-2-hydroxyphenyl]-5,7-dihydroxy-2-(4-hydroxyphenyl)chromen-4-one	*Hypericum perforatum, Trifolium pratense, Rosa canina, Glycyrrhiza glabra, Rhus coriaria*	-8.6
FPPS	Strictinin	$C_{27}H_{22}O_{18}$	[(10S,11R,12R,13S,15R)-3,4,5,11,12,21,22,23-octahydroxy-8,18-dioxo-9,14,17-trioxatetracyclo[17.4.0.$0^{2,7}$.$0^{10,15}$]tricosa-1(23),2,4,6,19,21-hexaen-13-yl] 3,4,5-trihydroxybenzoate	*Juglans regia*	-10.1
	cucurbitacin I 2-O-beta-D-glucopyranoside	$C_{36}H_{52}O_{12}$	(8S,9R,10R,13R,14S,16R,17R)-17-[(E,2R)-2,6-dihydroxy-6-methyl-3-oxohept-4-en-2-yl]-16-hydroxy-4,4,9,13,14-pentamethyl-2-[(2S,3R,4S,5S,6R)-3,4,5-trihydroxy-6-(hydroxymethyl)oxan-2-yl]oxy-8,10,12,15,16,17-hexahydro-7H-cyclopenta[a]phenanthrene-3,11-dione	*Citrullus colocynthis*	-9.7
	Corilagin	$C_{27}H_{24}O_{18}$	[(1S,19R,21S,22R,23R)-6,7,8,11,12,13,22,23-octahydroxy-3,16-dioxo-2,17,20-trioxatetracyclo[17.3.1.$0^{4,9}$.$0^{10,15}$]tricosa-4,6,8,10,12,14-hexaen-21-yl] 3,4,5-trihydroxybenzoate	*Terminalia chebula*	-9.6
	Amentoflavone	$C_{30}H_{18}O_{10}$	8-[5-(5,7-dihydroxy-4-oxochromen-2-yl)-2-hydroxyphenyl]-5,7-dihydroxy-2-(4-hydroxyphenyl)chromen-4-one	*Hypericum perforatum, Trifolium pratense, Rosa canina, Glycyrrhiza glabra, Rhus coriaria*	-9.6
	Hinokiflavone	$C_{30}H_{18}O_{10}$	6-[4-(5,7-dihydroxy-4-oxochromen-2-yl)phenoxy]-5,7-dihydroxy-2-(4-hydroxyphenyl)chromen-4-one	*Rhus coriaria*	-9.5

	luteolin-7-O-[beta-D-glucuronosyl-(1->2)-beta-D-glucuronide]	$C_{27}H_{26}O_{18}$	(2S,3S,4S,5R,6R)-6-[(2S,3R,4S,5S,6S)-6-carboxy-2-[2-(3,4-dihydroxyphenyl)-5-hydroxy-4-oxochromen-7-yl]oxy-4,5-dihydroxyoxan-3-yl]oxy-3,4,5-trihydroxyoxane-2-carboxylic acid	*Verbena officinalis*	-9.5
	Eriocitrin	$C_{27}H_{32}O_{15}$	(2S)-2-(3,4-dihydroxyphenyl)-5-hydroxy-7-[(2S,3R,4S,5S,6R)-3,4,5-trihydroxy-6-[[(2R,3R,4R,5R,6S)-3,4,5-trihydroxy-6-methyloxan-2-yl]oxymethyl]oxan-2-yl]oxy-2,3-dihydrochromen-4-one	*Ziziphus jujuba,* *Citrus Bergamia Risso*	-9.4
	Isorhoifolin	$C_{27}H_{30}O_{14}$	5-hydroxy-2-(4-hydroxyphenyl)-7-[(2S,3R,4S,5S,6R)-3,4,5-trihydroxy-6-[[(2R,3R,4R,5R,6S)-3,4,5-trihydroxy-6-methyloxan-2-yl]oxymethyl]oxan-2-yl]oxychromen-4-one	*Chrysanthemum morifolium,* *Rosmarinus officinalis*	-9.4
	Procyanidin B2	$C_{30}H_{26}O_{12}$	(2R,3R)-2-(3,4-dihydroxyphenyl)-8-[(2R,3R,4R)-2-(3,4-dihydroxyphenyl)-3,5,7-trihydroxy-3,4-dihydro-2H-chromen-4-yl]-3,4-dihydro-2H-chromene-3,5,7-triol	*Tilia cordata, Rheum ribes*	-9.2
	Silymarin	$C_{25}H_{22}O_{10}$	3,5,7-trihydroxy-2-[3-(4-hydroxy-3-methoxyphenyl)-2-(hydroxymethyl)-2,3-dihydro-1,4-benzodioxin-6-yl]-2,3-dihydrochromen-4-one	*Ephedra alata*	-9.2
	3,4,5-tricaffeoylquinic acid	$C_{34}H_{30}O_{15}$	(3R,5R)-3,4,5-tris[[(E)-3-(3,4-dihydroxyphenyl)prop-2-enoyl]oxy]-1-hydroxycyclohexane-1-carboxylic acid	*Chrysanthemum morifolium*	-9.2
	pelargonidin 3-O-rutinoside betaine	$C_{27}H_{30}O_{14}$	5-hydroxy-2-(4-hydroxyphenyl)-3-[(2S,3R,4S,5S,6R)-3,4,5-trihydroxy-6-[[(2R,3R,4R,5R,6S)-3,4,5-trihydroxy-6-methyloxan-2-yl]oxymethyl]oxan-2-yl]oxychromen-7-one	*Cornus mas*	-9.1
NMT	Chelidimerine	$C_{43}H_{32}N_2O_9$	1-[(23S)-24-methyl-5,7,18,20-tetraoxa-24-azahexacyclo[11.11.0.$0^{2,10}$.$0^{4,8}$.$0^{14,22}$.$0^{17,21}$]tetracosa-1(13),2,4(8),9,11,14(22),15,17(21)-octaen-23-yl]-3-(24-methyl-5,7,18,20-tetraoxa-24-azahexacyclo[11.11.0.$0^{2,10}$.$0^{4,8}$.$0^{14,22}$.$0^{17,21}$]tetracosa-1(13),2,4(8),9,11,14(22),15,17(21)-octaen-23-yl)propan-2-one	*Chelidonium majus*	-14.1
	Friedelin	$C_{30}H_{50}O$	(4R,4aS,6aS,6aS,6bR,8aR,12aR,14aS,14bS)-4,4a,6a,6b,8a,11,11,14a-octamethyl-2,4,5,6,6a,7,8,9,10,12,12a,13,14,14b-tetradecahydro-1H-picen-3-one	*Albizia lebbeck, Cassia fistula*	-12.7
	Hypericin	$C_{30}H_{16}O_8$	9,11,13,16,18,20-hexahydroxy-5,24-dimethyloctacyclo[13.11.1.$1^{2,10}$.$0^{3,8}$.$0^{4,25}$.$0^{19,27}$.$0^{21,26}$.$0^{14,28}$]octacosa-1(26),2,4(25),5,8,10,12,14(28),15(27),16,18,20,23-tridecaene-7,22-dione	*Hypericum perforatum*	-12.5
	Pseudohypericin	$C_{30}H_{16}O_9$	9,11,13,16,18,20-hexahydroxy-5-(hydroxymethyl)-24-methyloctacyclo[13.11.1.$1^{2,10}$.$0^{3,8}$.$0^{4,25}$.$0^{19,27}$.$0^{21,26}$.$0^{14,28}$]octacosa-1(26),2,4(25),5,8,10,12,14(28),15(27),16,18,20,23-tridecaene-7,22-dione	*Hypericum perforatum*	-11.7
	Bismahanine	$C_{46}H_{48}N_2O_4$	10-[9-hydroxy-3,5-dimethyl-3-(4-methylpent-3-enyl)-11H-pyrano[3,2-a]carbazol-8-yl]-3,5-dimethyl-3-(4-methylpent-3-enyl)-11H-pyrano[3,2-a]carbazol-9-ol	*Murraya koenigii*	-11.7

Eucalbanin A	$C_{48}H_{30}O_{30}$	[(10R,11S,12R,15R)-3,4,5,13,21,22,23-heptahydroxy-8,18-dioxo-11-(3,4,5-trihydroxybenzoyl)oxy-9,14,17-trioxatetracyclo[17.4.0.0^{2,7}.0^{10,15}]tricosa-1(23),2,4,6,19,21-hexaen-12-yl] 3,4,5-trihydroxy-2-[(6,13,14-trihydroxy-3,10-dioxo-2,9-dioxatetracyclo[6.6.2.0^{4,16}.0^{11,15}]hexadeca-1(15),4,6,8(16),11,13-hexaen-7-yl)oxy]benzoate	*Juglans regia*	-11.6
Amentoflavone	$C_{30}H_{18}O_{10}$	8-[5-(5,7-dihydroxy-4-oxochromen-2-yl)-2-hydroxyphenyl]-5,7-dihydroxy-2-(4-hydroxyphenyl)chromen-4-one	*Hypericum perforatum, Trifolium pratense, Rosa canina, Glycyrrhiza glabra, Rhus coriaria*	-11.6
Protohypericin	$C_{30}H_{18}O_8$	9,11,13,16,18,20-hexahydroxy-5,24-dimethylheptacyclo[13.11.1.1^{2,10}.0^{3,8}.0^{19,27}.0^{21,26}.0^{14,28}]octacosa-1,3,5,8,10,12,14(28),15(27),16,18,20,23,25-tridecaene-7,22-dione	*Hypericum perforatum*	-11.5
Dioscin	$C_{45}H_{72}O_{16}$	(2S,3R,4R,5R,6S)-2-[(2R,3S,4S,5R,6R)-4-hydroxy-2-(hydroxymethyl)-6-[(1S,2S,4S,5'R,6R,7S,8R,9S,12S,13R,16S)-5',7,9,13-tetramethylspiro[5-oxapentacyclo[10.8.0.0^{2,9}.0^{4,8}.0^{13,18}]icos-18-ene-6,2'-oxane]-16-yl]oxy-5-[(2S,3R,4R,5R,6S)-3,4,5-trihydroxy-6-methyloxan-2-yl]oxyoxan-3-yl]oxy-6-methyloxane-3,4,5-triol	*Tribulus terrestris*	-11.5
3,8'-Biapigenin	$C_{30}H_{18}O_{10}$	8-[5-(5,7-dihydroxy-4-oxochromen-2-yl)-2-hydroxyphenyl]-5,7-dihydroxy-2-(4-hydroxyphenyl)chromen-4-one	*Hypericum perforatum*	-11.4
Naphthalene, 2-(1-adamantyl)-7-(2-adamantyl)-	$C_{30}H_{36}$	1-[7-(2-adamantyl)naphthalen-2-yl]adamantane	*Lawsonia inermis*	-11.3
Fern-7-ene	$C_{30}H_{50}$	(3R,3aR,5aS,7aS,11aS,11bR,13aS)-3a,5a,8,8,11a,13a-hexamethyl-3-propan-2-yl-1,2,3,4,5,7,7a,9,10,11,11b,12,13,13b-tetradecahydrocyclopenta[a]chrysene	*Adiantum capillus-veneris*	-11.2
Chebulinic acid	$C_{41}H_{32}O_{27}$	2-[(4R,5S,7R,8R,11S,12S,13S,21S)-13,17,18-trihydroxy-2,10,14-trioxo-5,21-bis[(3,4,5-trihydroxybenzoyl)oxy]-7-[(3,4,5-trihydroxybenzoyl)oxymethyl]-3,6,9,15-tetraoxatetracyclo[10.7.1.1^{4,8}.0^{16,20}]henicosa-1(19),16(20),17-trien-11-yl]acetic acid	*Terminalia chebula*	-11.2

GP63, Glycoprotein 63; FPPS, farnesyl diphosphate synthase; NMT, N-myristoyltransferase.

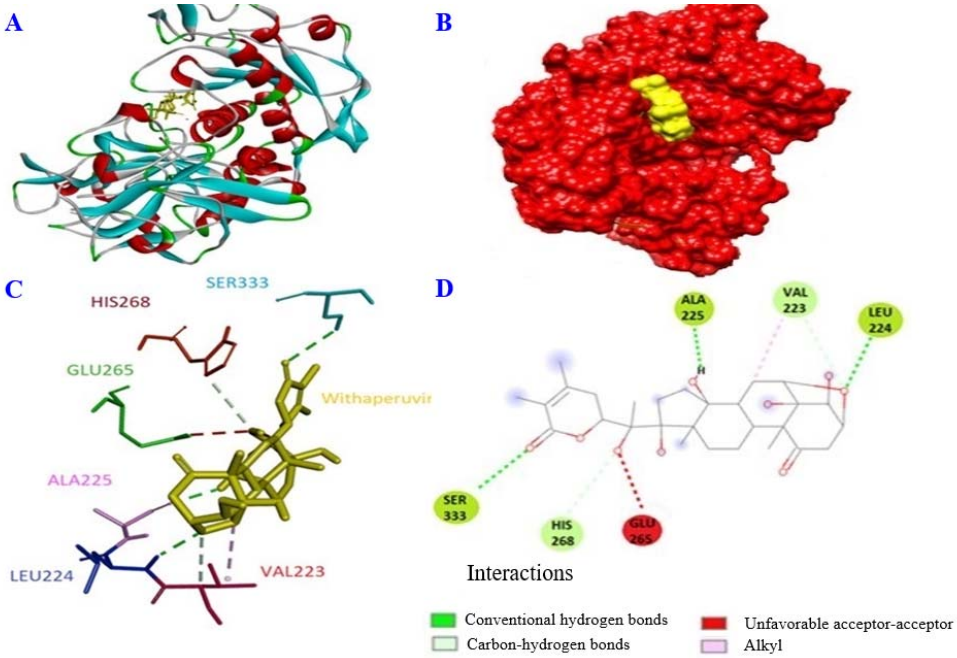

Fig. 5. Interaction of withaperuvin D with GP63 protein. (A) Solid ribbon display of withaperuvin D interaction with GP63 protein. The α-helices, β-sheets, and linker sites of the protein are depicted in red, blue, and green, respectively. Moreover, the ligand is illustrated in mustard. (B) 3D surface of withaperuvin D and GP63 interaction. Withaperuvin D is shown in yellow, and GP63 is demonstrated in red. (C) 3D interface of amino acids involved in the interaction. Withaperuvin D is displayed in mustard, and GP63 amino acids are presented in dark red, medium blue, plum, green, violet red, and blue. (D) Different kinds of bonds between important amino acids involved in interaction from GP63, and withaperuvin D are delineated in the 2D surface. Conventional hydrogen bonds, unfavorable acceptor-acceptor, alkyl, and carbon-hydrogen bonds are presented in green, red, pink, and sky blue, respectively. GP63, Glycoprotein 63.

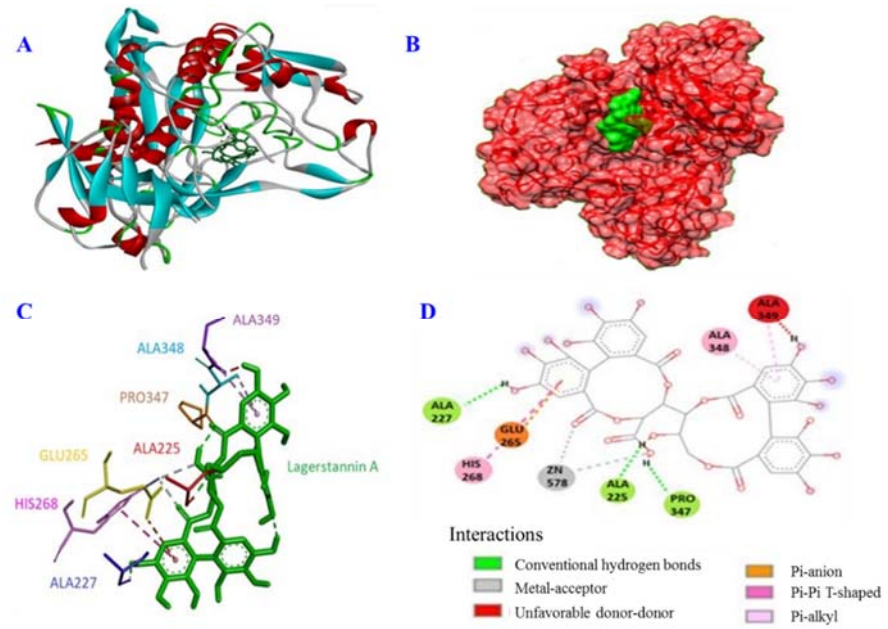

Fig. 6. Interaction of lagerstannin A with the GP63 protein. (A) Solid ribbon display of lagerstannin A interaction with GP63 protein. The α-helices, β-sheets, and linker sites of the protein are depicted in red, blue, and green, respectively. Thus, the ligand is illustrated in green. (B) 3D surface of lagerstannin A and GP63 interaction. Lagerstannin A is shown in green, and GP63 is demonstrated in red. (C) 3D interface of amino acids involved in the interaction. Lagerstannin A is displayed in green, and GP63 amino acids are presented in dark red, medium blue, purple, plum, yellow, brown, and blue. (D) Different kinds of bonds among important amino acids involved in interaction from GP63, and lagerstannin A are delineated in the 2D surface. Conventional hydrogen bonds, unfavorable donor-donor, pi-alkyl, pi-pi T-shaped, metal-acceptor, and pi-anion are presented in green, red, pink, deep pink, gray, and orange, respectively. GP63, Glycoprotein 63.

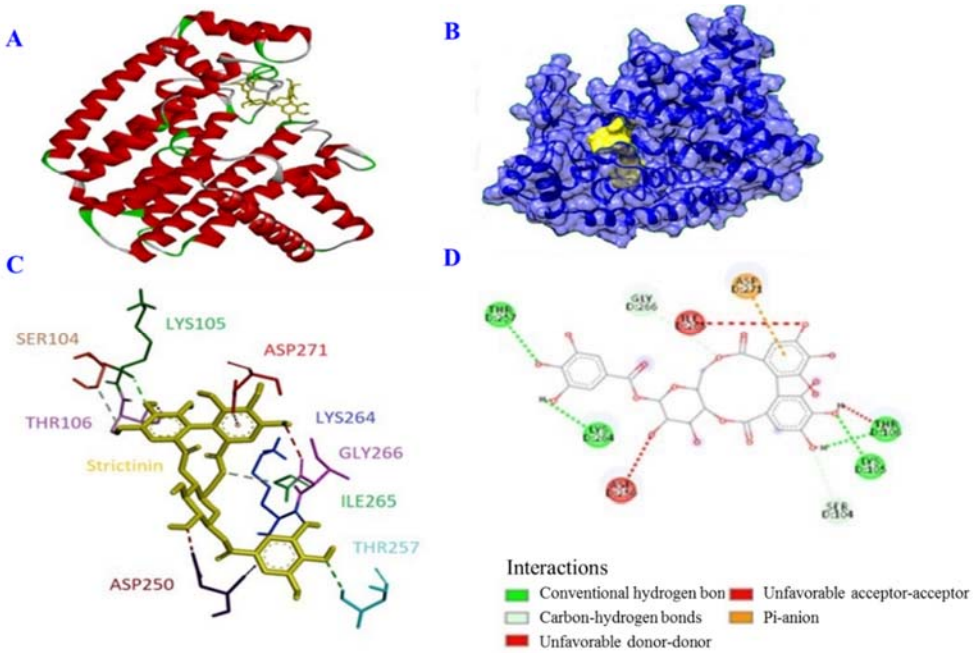

Fig. 7. Interaction of strictinin with FPPS protein. (A) Solid ribbon display of strictinin interaction with FPPS protein. The α-helices and linker sites of the protein are depicted in red and green, respectively. Therefore, the ligand is illustrated in yellow. (B) 3D surface of strictinin and FPPS interaction. Strictinin is shown in yellow, and FPPS is demonstrated in blue. (C) 3D interface of amino acids involved in the interaction. Strictinin is displayed in yellow, and FPPS amino acids are presented in dark red, medium blue, violet red, sea green, dark green, purple, plum, brown, and blue. (D) Different kinds of bonds between important amino acids involved in interaction from FPPS and strictinin are delineated in the 2D surface. Conventional hydrogen bonds, unfavorable acceptor-acceptor interactions, unfavorable donor-donor interactions, pi-anion interactions, and carbon-hydrogen bonds are represented in green, red, orange, sky blue, and blue, respectively. FPPS, Farnesyl diphosphate synthase.

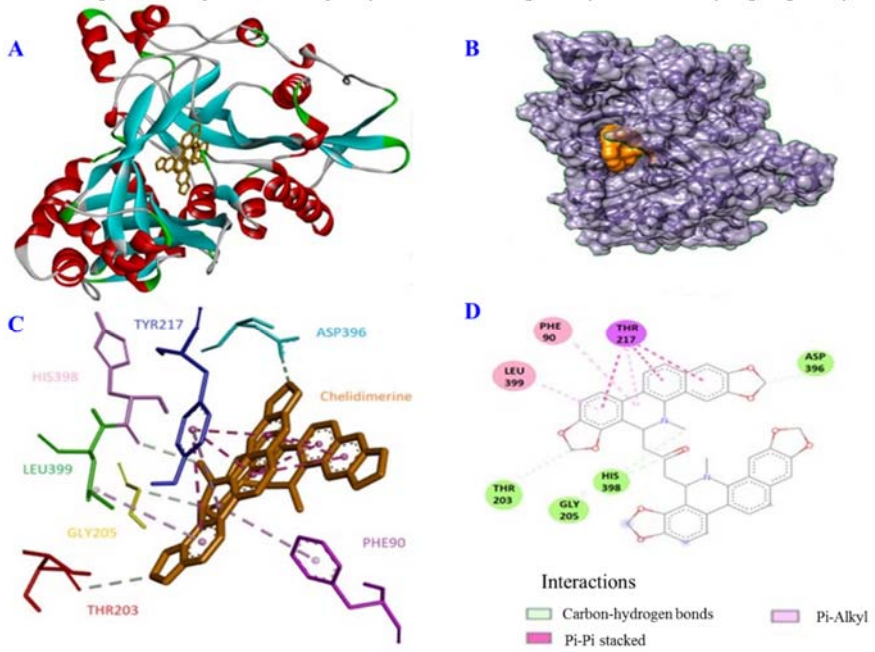

Fig. 8. Interaction of chelidimerine with NMT protein. (A) Solid ribbon display of chelidimerine interaction with NMT protein. The α-helices, β-sheets, and linker sites of the protein are depicted in red, blue, and green, respectively. Thus, the ligand is illustrated in brown. (B) 3D surface of chelidimerine and NMT interaction. Chelidimerine is shown in brown, and NMT is demonstrated in medium purple. (C) 3D interface of amino acids involved in the interaction. Chelidimerine is displayed in brown, and NMT amino acids are presented in dark red, medium blue, dark green, purple, plum, yellow, and blue. (D) Different kinds of bonds between important amino acids involved in interaction from NMT and chelidimerine are delineated in the 2D surface. pi-Alkyl, pi-pi stacked, and carbon-hydrogen bonds are presented in pink, deep pink, and sky blue, respectively. NMT, N-myristoyltransferase.

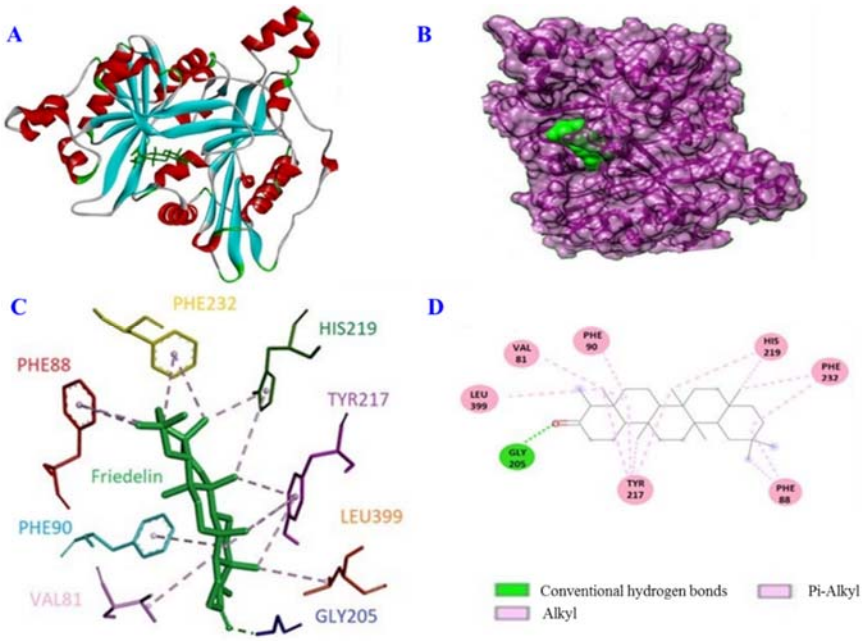

Fig. 9. Interaction of friedelin with the NMT protein. (A) Solid ribbon display of friedelin interaction with NMT protein. The α-helices, β-sheets, and linker sites of the protein are depicted in red, blue, and green, respectively. Therefore, the ligand is illustrated in dark green. (B) 3D surface of friedelin and NMT interaction. Friedelin is shown in dark green, and NMT is demonstrated in dark magenta. (C) 3D interface of amino acids involved in the interaction. Friedelin is displayed in dark green, and NMT amino acids are presented in dark red, medium blue, forest green, mustard, purple, plum, brown, and blue. (D) Different kinds of bonds between important amino acids involved in interaction from NMT and friedelin are delineated in the 2D surface. pi-alkyl, alkyl, and conventional hydrogen bonds are presented in pink, pink, and green, respectively. NMT, N-myristoyltransferase.

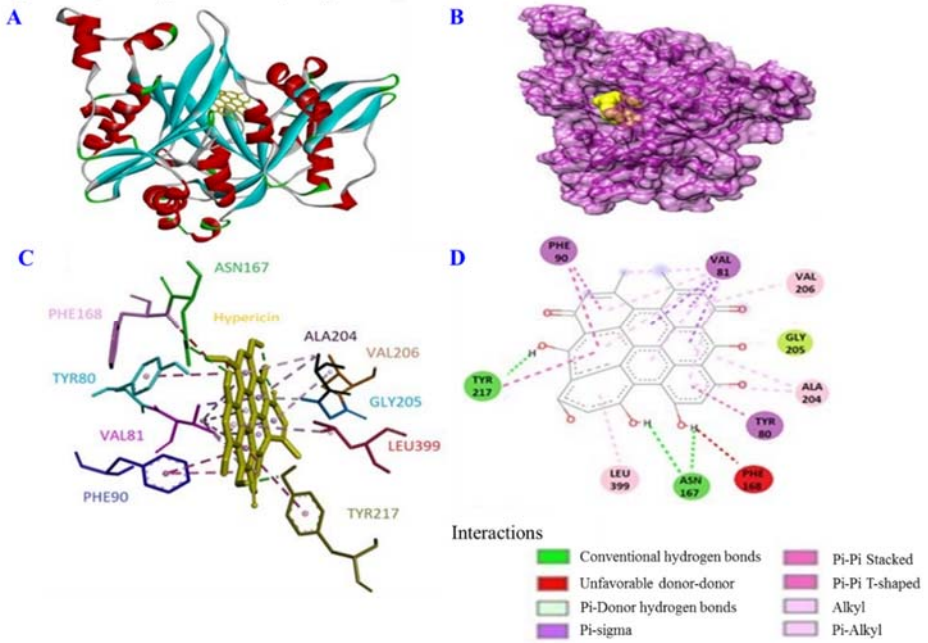

Fig. 10. Interaction of hypericin with the NMT protein. (A) Solid ribbon display of hypericin interaction with NMT protein. The α-helices, β-sheets, and linker sites of the protein are depicted in red, blue, and green, respectively. Thus, the ligand is illustrated in mustard. (B) 3D surface of hypericin and NMT interaction. Hypericin is shown in mustard, and NMT is demonstrated in orchid. (C) 3D interface of amino acids involved in the interaction. Hypericin is displayed in mustard, and NMT amino acids are presented in dark olive green, cyan, dark red, medium blue, green, brown, purple, plum, and blue. (D) Different kinds of bonds between important amino acids involved in interaction from NMT and hypericin are delineated in the 2D surface. pi-alkyl, alkyl, and conventional hydrogen bonds are presented in pink, pink, and green, respectively. Conventional hydrogen bonds, unfavorable donor-donor, pi-sigma, pi-pi stacked, pi-pi T-shaped, alkyl, pi-alkyl, and pi-donor hydrogen bonds are presented in green, red, purple, magenta, magenta, pink, pink, and sky blue, respectively. NMT, N-myristoyltransferase.

Table 3. Affinity analysis of common compounds with high affinity for GP63, FPPS, and NMT proteins.

protein name	Common compounds	Docking score (kcal/mol)
GP63	Amentoflavone	-8.6
	Protohypericin	-8.4
	Luteolin 3'-o- glucuronide	-8.0
FPPS	Amentoflavone	-9.6
	Protohypericin	-8.7
	Luteolin 3'-o- glucuronide	-8.3
NMT	Amentoflavone	-11.6
	Protohypericin	-9.6
	Luteolin 3'-o- glucuronide	-11.5

GP63, Glycoprotein 63; FPPS, farnesyl diphosphate synthase; NMT, N-myristoyltransferase.

Moreover, the presence of benzene and cycloalkane rings is fundamental for the hydrophobic interaction of pi-pi and pi-alkyl types with amino acids His268, Glu265, Val233, Ala348, and Ala349, and a docking score of -9.2 kcal/mol.

The interaction of the bisphosphonate compound that restrains the dynamic location of FPPS protein is as follows: it has four hydrogen bonds with amino acids Thr43, Tyr49, Asn51, and Gln91, with separations of 3.180, 2.545, 2.338, and 2.263. It has two electrostatic interactions with Lys48 and Arg51, with a docking score of -6.6 kcal/mol. Phenylbutazone exhibited the subsequent discernible interactions with the dynamic sites of the FPPS protein: hydrogen holding with amino acid Tyr 211, cation electrostatic interaction with amino acid Arg 51, and hydrophobic interaction with amino acid Lys 207. Its docking score was about -6.3 kcal/mol. In stable hydrogen interaction of strytinin with amino acids Asp250, Gly266, Ile265, Asp271, Thr106, Lys264, Ser104, Thr257, and Lys105 in the active site of FPPS protein, phenolic OH groups and oxygen played an important role. In addition, the benzene ring played a role in the hydrophobic interaction with Asp271 and its docking score was about -10.1 kCal/mol.

The intelligence of the bisphosphonate compound hindering the NMT protein in its dynamic location is as follows. It had four hydrogen bonds with amino acids Glu72, Val71, Tyr335, and His209, with separations of 3.040, 3.698, 2.204, and 3.336. It had a hydrophobic interaction with Phe80 and an electrostatic interaction with Asp386 and Tyr207, with a docking score of -6.4 kcal/mol. The presence of benzene rings and alkyl (aliphatic) groups in the hydrophobic interaction of the active site of NMT protein with Try217, Phe90, and Leu399 amino acids is required. Furthermore, the hydrogen interaction between chylidimarin and the amino acids Asp396, Gly205, and His398 requires the presence of oxygen and nitrogen groups; this interaction had a docking score of -14.1 kcal/mol. Similarly, the hydrogen interaction between Friedlin and the amino acid Gly205 requires the presence of a carbonyl group; the docking score for this interaction was -12.7 kcal/mol. In hypericin, the presence of oxygen atoms in the structure of the compound in the form of carbonyl, and available to form a hydrogen bond with amino acids Tyr217, Phe168, Asn167 and Gly205 is necessary, and its docking score was -12.5 kcal/mol. Piperidinylindole has four hydrogen bonds with amino acids Thr193, Phe158, and Leu411. It has hydrophobic interactions with Gly195, Ala194, Val71, and Ieu159 amino acids. The desired compound had an electrostatic interaction of pi-sulfur, hydrophobic, and hydrogen type with the amino acid TYR70. The docking score of this compound with NMT is about -9.2 kcal/mol.

As previously stated, the proposed compounds form extremely strong bonds, including covalent, hydrogen, and ionic bonds, with specific amino acids located within the active site of the specified proteins. Furthermore, these compounds completely encase the active site of the protein, preventing it from forming connections with other ligands and constraining its activity (Figs. 5-10). The molecular docking of our proposed compounds was compared with several leishmaniasis inhibitors presented in several articles in Table 4. Redocking was done by the main inhibitor, bisphosphonate, for all three proteins, and the RMSD value of all interactions was less than 2 Å.

Table 4. Comparing the molecular docking of our proposed compounds with some blockers presented in several articles.

Protein name	Compound	Docking score (kcal/mol)	Blocker	Docking score (kcal/mol)	Reference
GP63	Withaperuvin D	-9.2	Bisphosphonate	-5.7	(48)
	Lagerstannin A	-9.2	Podocarpusflavone A	-8.5	(49)
	Physagulin D	-9.1	bipinnatone A	-8.0	(26)
	Luteolin 7-O-(6"-malonylglucoside)	-9.0	medicagenina	-8.0	(26)
FPPS	Strictinin	-10.1	Bisphosphonate	-6.6	(48)
	cucurbitacin I 2-O-beta-D-glucopyranoside	-9.7	Phenylbutazone	-6.3	(50)
			Podocarpusflavone B	-8.4	(49)
	Corilagin	-9.6	3-Fluoro-1-(2-hydroxy-2,2-diphosphonoethyl)pyridinium	-6.4	(27)
	Hinokiflavone	-9.5			
NMT	Chelidimerine	-14.1	Bisphosphonate	-6.4	(48)
	Friedelin	-12.7	Piperidinylindole	-9.2	(51)
	Hypericin	-12.5			(9)
	Bismahanine	-11.7	Amphotericin B	-5.0	(52)
			Thienopyrimidine	-4.6	(9)

GP63, Glycoprotein 63; FPPS, farnesyl diphosphate synthase; NMT, N-myristoyltransferase.

Based on Table 4, the binding scores of compounds presented in this study were higher than other blockers proposed from the articles, considering that the blockers with the highest binding energy were selected from these articles, and still have weaker binding with *Leishmania* protein than the compounds proposed in the present research. Therefore, the bond of these compounds will probably have little strength and stability in the body.

Results from the Lazar and WaytoDrug Databases

Results from Lazar and WaytoDrug are shown in Table 5.

Results from the SwissADME database

The physicochemical characteristics of medicinal compounds obtained from the database are shown in Table 6. Other characteristics of compounds, including lipophilicity, water solubility, and pharmacokinetics, are shown in Tables 7-9, respectively. Table 7 indicates that chelidimerine and friedelin compounds exhibited higher lipophilicity compared to others, resulting in superior absorption. Conversely, lagerstannin A and strictinin compounds, having the lowest lipophilicity, had the worst absorption capacity. LIPO (lipophilicity), SIZE, POLAR (polarity), INSOLU (insoluble), INSATU (Insaturated), and FLEX (flexibility) for each compound are shown in Fig. 11.

Results of MD simulation analysis

GP63/Withaperuvin D, FPPS/strictinin, NMT/chelidimerine, NMT/friedelin, and NMT/hypericin results from the docking analysis were refined using MD simulation. Finally, 1000 ns scale time MD simulations were performed to understand the stability of interactions. The study analyzed many plots (Figs. 12-19) such as RMSD, RMSF, Rg, PCA, MM/PBSA binding energy, and SASA. The compound lagerstamin A was excluded from the graphs because of its inherent instability.

RMSD

RMSD of backbone atoms was used to assess the overall structural stability of proteins. This reveals how significantly the protein shape changed from the original structure during the MD simulation. The RMSD value for GP63/withaperuvin D was in the range of 0.1 to 0.3 nm (Fig. 12A). Based on FPPS/strictinin results (Fig. 12B), the RMSD value was in the range of 0.1 to 0.5 nm. The RMSD values for the NMT/chelidimerine, NMT/friedelin, and NMT/hypericin proteins ranged from 0.10 to 0.22 nm (Fig. 12C). Figure 8 shows that the range of 50 to 100 ns has the lowest fluctuations, indicating the stability of interactions.

Table 5. Different characteristics of common and medicinal herbs with high affinity to GP63, FPPS, and NMT proteins.

Name of compound	Activity[1]	Carcinogenicity (mouse)[2]	Carcinogenicity (rat)[2]
Withaperuvin D	Antineoplastic, antieczematic, antidiabetic, lipoprotein disorders treatment, antipruritic, antineoplastic (breast cancer), antineoplastic (lung cancer), antimetastatic, apoptosis agonist.	Non-carcinogen	Non-carcinogen
Lagerstannin A	Anaphylatoxin receptor antagonist, TP53 expression enhancer, antineoplastic, cytostatic, anti-inflammatory, hepatoprotectant, apoptosis agonist, antifungal, anticarcinogenic, antibacterial, antieczematic, antioxidant, antiviral (herpes), hemostatic, antithrombotic, antianginal, caspase 8 stimulant.	Non-carcinogen	N/D
Strictinin	TP53 expression enhancer, hepatoprotectant, cytostatic, antineoplastic, apoptosis agonist, antioxidant, anticarcinogenic, anti-inflammatory, antiviral (herpes), hepatic disorders treatment, antineoplastic (non-Hodgkin's lymphoma), non-steroidal anti-inflammatory agent, immunostimulant, antifungal, membrane permeability inhibitor, antibacterial, antineoplastic (lung cancer), cardio protectant, anaphylatoxin receptor antagonist, caspase 8 stimulant	Non-carcinogen	N/D
Chelidimerine	Antineoplastic (multiple myeloma), antineurotic, antineoplastic alkaloid, antineoplastic (lymphoma), antineoplastic (solid tumors), antiprotozoal, antitussive	N/D	N/D
Friedelin	Apoptosis agonist, antineoplastic, antieczematic, mucomembranous protector, dermatologic, hepatic disorders treatment, antiinflammatory, antipruritic, antinociceptive, antiviral (influenza), prostate disorders treatment, antipsoriatic, antineoplastic (lung cancer), antiseborrheic, erythropoiesis stimulant, antineoplastic (melanoma), antiulcerative, lipid metabolism regulator, antineoplastic (breast cancer), dementia treatment, antiacne, menopausal disorders treatment, antimetastatic, antileukemic, antipruritic, antiprotozoal (leishmania), prostatic (benign) hyperplasia treatment, antineoplastic (thyroid cancer), antineoplastic (endocrine cancer), antineoplastic (ovarian cancer), alopecia treatment, vascular dementia treatment, antithrombotic	N/D	N/D
Hypericin	TP53 expression enhancer, antineoplastic, apoptosis agonist, kidney function stimulant, antiseptic, antimutagenic, nucleotide metabolism regulator, antihelmintic (nematodes), acute neurologic disorders treatment, erythropoiesis stimulant, antineoplastic (breast cancer), membrane integrity agonist, membrane permeability inhibitor, anaphylatoxin receptor antagonist, caspase 3 stimulant, antiseborrheic	Non-carcinogen	N/D
Amentoflavone	TP53 expression enhancer, antimutagenic, apoptosis agonist, antiseborrheic, antineoplastic, MAP kinase stimulant, antihemorrhagic, antineoplastic (breast cancer), anticarcinogenic, antiseptic, mucomembranous protector, free radical scavenger, antioxidant, kidney function stimulant, hepatoprotectant, antiinflammatory, antimycobacterial, antifungal, antiprotozoal (leishmania), antileukemic, antineoplastic (small cell lung cancer), antiviral (herpes), antihypercholesterolemic, caspase 3 stimulant, alopecia treatment	Non-carcinogen	Non-carcinogen
Protohypericin	TP53 expression enhancer, antineoplastic, antiseborrheic, antiseptic, apoptosis agonist, antimutagenic, mucomembranous protector, kidney function stimulant, anti-infective, antineoplastic (breast cancer), antihelmintic (nematodes), alopecia treatment, antieczematic, laxative, anti-helicobacter pylori, nucleotide metabolism regulator, antidyskinetic, acute neurologic disorders treatment, antiparasitic, anticarcinogenic, antineoplastic (lung cancer), hemostatic	N/D	N/D
Luteolin 3'-o-glucuronide	free radical scavenger, cardioprotectant, antihypercholesterolemic, chemopreventive, hepatoprotectant, anticarcinogenic, antioxidant, antiprotozoal (leishmania), antimutagenic, antineoplastic, skin whitener, antiinfective, antiviral (influenza), antiinflammatory, antifungal, apoptosis agonist, antitussive, antihemorrhagic, hepatic disorders treatment, antithrombotic, antiuremic, antiulcerative, antibacterial, antitoxic, caspase 8 stimulant, antidote, antidiabetic, antimycobacterial, antinociceptive	N/D	Non-carcinogen

1, the activity of each active substance gained from the pass online database (http://www.pharmaexpert.ru/passonline/index.php); 2, the blood-brain barrier, carcinogenicity, and maximum recommended daily dose prediction were obtained from the Lazar database (https://lazar.in-silico.ch); GP63, glycoprotein 63; FPPS, farnesyl diphosphate synthase; NMT, N-myristoyltransferase; N/D, not defined.

Table 6. Different physicochemical properties of common medicinal herbal compounds with high affinity to GP63, FPPS, and NMT proteins.

Compound name	Formula	Molecular weight (g/mol)	Number of heavy atoms	Number of aromatic heavy atoms	Fraction Csp3	Number of rotatable bonds	Number of H-bond acceptors	Number of H-bond donors	Molar refractivity	TPSA
Withaperuvin D	$C_{28}H_{40}O_9$	520.61	37	0	0.86	2	9	5	131.56	153.75 Å²
Lagerstannin A	$C_{34}H_{24}O_{23}$	800.54	57	24	0.15	2	23	14	179.36	405.49 Å²
Strictinin	$C_{27}H_{22}O_{18}$	634.45	45	18	0.22	3	18	11	141.85	155.52 Å²
Chelidimerine	$C_{43}H_{32}N_2O_9$	720.72	54	32	0.23	4	9	0	205.9	97.39 Å²
Friedelin	$C_{30}H_{50}O$	426.72	31	0	0.97	0	1	0	134.39	17.07 Å²
Hypericin	$C_{30}H_{16}O_8$	504.44	38	22	0.07	0	8	6	144.83	155.52 Å²
Amentoflavone	$C_{30}H_{18}O_{10}$	538.46	40	32	0	3	10	6	146.97	181.80 Å²
Protohypericin	$C_{30}H_{18}O_8$	506.46	38	20	0.07	0	8	6	144.53	155.52 Å²
Luteolin 3'-o-glucuronide	$C_{21}H_{18}O_{12}$	462.36	33	16	0.24	4	12	7	108.74	207.35 Å²

TPSA, Topological polar surface area; GP63, glycoprotein 63; FPPS, farnesyl diphosphate synthase; NMT, N-myristoyltransferase.

Table 7. Different lipophilicity characteristics of common medicinal herbal compounds with high affinity to GP63, FPPS, and NMT proteins.

Lipophilicity	Log $P_{o/w}$ (iLOGP)	Log $P_{o/w}$ (XLOGP3)	Log $P_{o/w}$ (WLOGP)	Log $P_{o/w}$ (MLOGP)	Log $P_{o/w}$ (SILICOS-IT)	Consensus Log $P_{o/w}$
Withaperuvin D	1.8	-0.35	0.92	0.48	2.06	0.98
Lagerstannin A	-0.39	0.71	0.39	-2.97	-2.17	-0.89
Strictinin	0.92	0.07	-0.3	-2.42	-2.15	-0.77
Chelidimerine	5.31	7.67	6.86	4.02	7.03	6.18
Friedelin	4.52	9.8	8.46	6.92	7.52	7.44
Hypericin	3.1	5.71	5.76	1.36	5.37	4.26
Amentoflavone	3.06	5.04	5.13	0.25	4.61	3.62
Protohypericin	1.76	3.79	3.82	1.33	4.71	3.08
Luteolin 3'-o-glucuronide	1.69	1.22	-0.15	-2.12	-0.57	0.01

GP63, glycoprotein 63; FPPS, farnesyl diphosphate synthase; NMT, N-myristoyltransferase.

Table 8. Different water solubility characteristics of common medicinal herbal compounds with high affinity to GP63, FPPS, and NMT proteins.

Compound name	Log *S* (ESOL)	Solubility	Class	Log *S*	Solubility	Class	Log *S* (SILICOS-IT)	Solubility	Class
Withaperuvin D	-2.72	1.00e+00 mg/mL; 1.93e-03 mol/L	Soluble	-2.42	1.99e+00 mg/mL; 3.83e-03 mol/L	Soluble	-2.67	1.11e+00 mg/mL; 2.12e-03 mol/L	Soluble
Lagerstannin A	-5.43	2.97e-03 mg/mL; 3.71e-06 mol/L	Moderately soluble	-8.8	1.26e-06 mg/mL; 1.57e-09 mol/L	Poorly soluble	-1.34	3.64e+01 mg/mL; 4.55e-02 mol/L	Soluble
Strictinin	-3.92	7.70e-02 mg/mL	Soluble	-6.15	4.52e-04 mg/mL; 7.12e-07 mol/l	Poorly soluble	-0.51	1.95e+02 mg/mL; 3.07e-01 mol/L	Soluble
Chelidimerine	-9.32	3.49e-07 mg/mL; 4.84e-10 mol/L	Poorly soluble	-9.56	2.01e-07 mg/mL; 2.78e-10 mol/L	Poorly soluble	-12.12	5.40e-10 mg/mL; 7.50e-13 mol/L	Insoluble
Friedelin	-8.66	9.34e-07 mg/mL; 2.19e-09 mol/L	Poorly soluble	-10.08	3.56e-08 mg/mL; 8.33e-11 mol/l	Insoluble	-7.88	5.66e-06 mg/mL; 1.33e-08 mol/L	Poorly soluble
Hypericin	-6.99	5.12e-05 mg/mL; 1.02e-07 mol/L	Poorly soluble	-8.74	9.13e-07 mg/mL; 1.81e-09 mol/L	Poorly soluble	-7.17	3.37e-05 mg/mL; 6.68e-08 mol/L	Poorly soluble
Amentoflavone	-6.75	9.63e-05 mg/mL; 1.79e-07 mol/L	Poorly soluble	-8.6	1.36e-06 mg/mL; 2.52e-09 mol/L	Poorly soluble	-8.7	1.07e-06 mg/mL; 1.98e-09 mol/L	Poorly soluble
Protohypericin	-5.76	8.86e-04 mg/mL; 1.75e-06 mol/L	Moderately soluble	-6.75	9.01e-05 mg/mL; 1.78e-07 mol/L	Poorly soluble	-6.43	1.89e-04 mg/mL; 3.73e-07 mol/L	Poorly soluble
Luteolin 3'-o-glucuronide	-3.57	1.24e-01 mg/mL; 2.69e-04 mol/L	Soluble	-5.17	3.11e-03 mg/mL; 6.74e-06 mol/L	Moderately soluble	-1.63	1.08e+01 mg/mL; 2.33e-02 mol/L	Soluble

GP63, glycoprotein 63; FPPS, farnesyl diphosphate synthase; NMT, N-myristoyltransferase.

Table 9. Different pharmacokinetic characteristics of common medicinal herbal compounds with high affinity to GP63, FPPS, and NMT proteins.

Compound name	GI absorption	BBB permeant	P-gp substrate	CYP1A2 inhibitor	CYP2C19 inhibitor	CYP2C9 inhibitor	CYP2D6 inhibitor	CYP3A4 inhibitor	Log K_p (skin permeation)
Withaperuvin D	Low	No	Yes	No	No	No	No	No	-9.72 cm/s
Lagerstannin A	Low	No	Yes	No	No	No	No	No	-10.58 cm/s
Strictinin	Low	No	Yes	No	No	No	No	No	No
Chelidimerine	Low	No	Yes	No	No	No	No	Yes	-5.25 cm/s
Friedelin	Low	No	No	No	No	No	No	No	No
Hypericin	Low	No	No	No	Yes	Yes	No	No	-5.32 cm/s
Amentoflavone	Low	No	Yes	No	No	No	No	Yes	-6.01 cm/s
Protohypericin	Low	No	No	No	Yes	Yes	No	No	-6.70 cm/s
Luteolin 3'-o-glucuronide	Low	No	Yes	No	No	No	No	No	-8.25 cm/s

GP63, glycoprotein 63; FPPS, farnesyl diphosphate synthase; NMT, N-myristoyltransferase; GI, gastrointestinal; BBB, blood-brain barrier; P-gp, permeability glycoprotein.

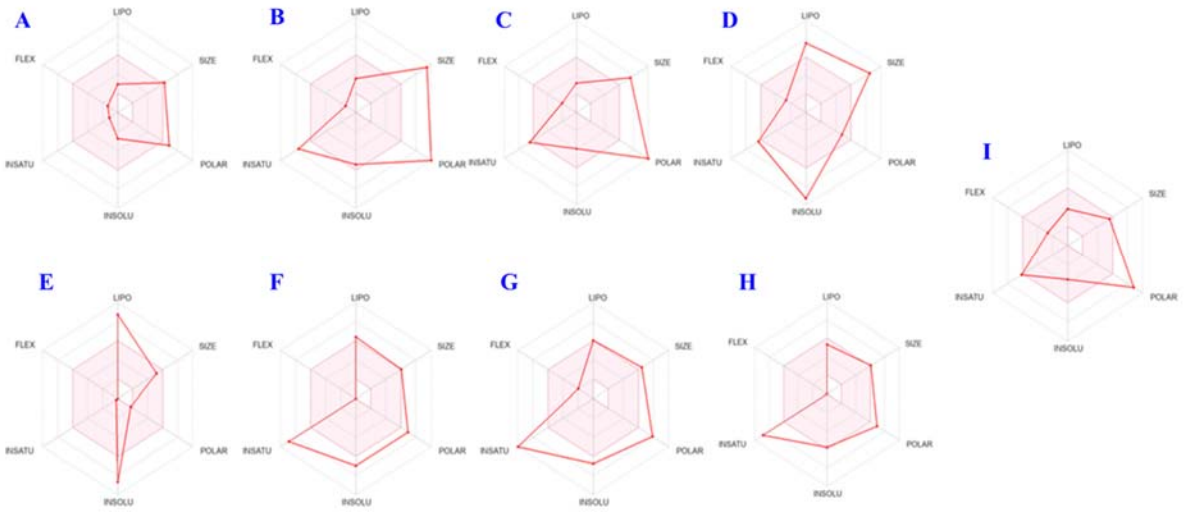

Fig. 11. Lipophilicity, size, polarity, insolubility, insaturation, and flexibility features of compounds. The colored zone is the suitable physicochemical space for oral bioavailability. Herbal compounds include (A) withaperuvin D; (B) lagerstamin A; (C) strictinin; (D) chelidimerine; (E) friedelin; (F) hypericin; (G) amentoflavone; (H) protohypericin; and (I) luteolin 3'-o-glucuronide.

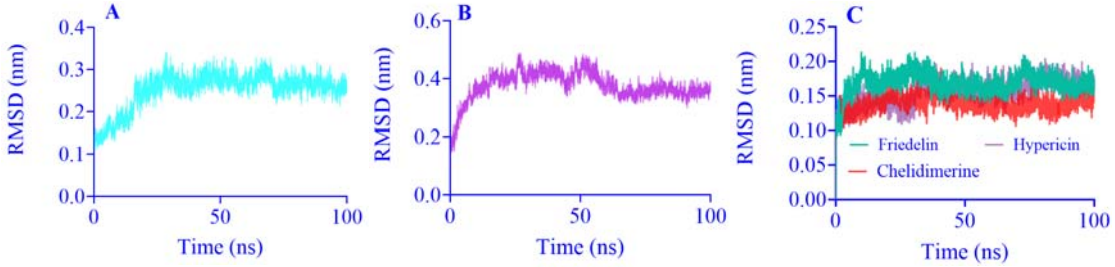

Fig. 12. The RMSD diagram of (A) GP63/withaperuvin D; (B) FPPS/strictinin; (C) NMT/chelidimerine, NMT/friedelin, and NMT/hypericin. GP63, Glycoprotein 63; FPPS, farnesyl diphosphate synthase; NMT, N-myristoyltransferase.

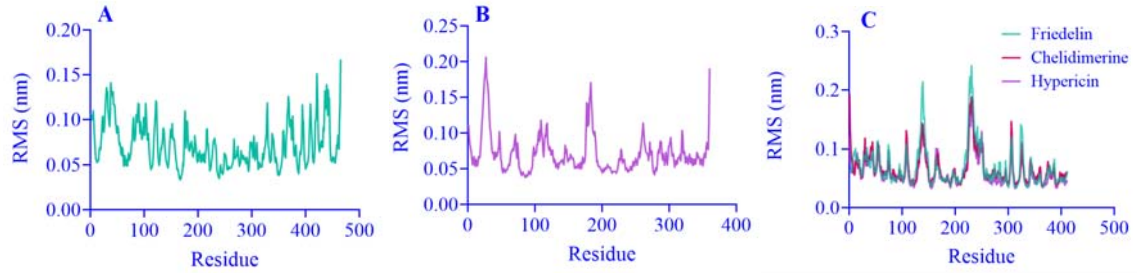

Fig. 13. RMSF diagram of (A) GP63/withaperuvin D; (B) FPPS/strictinin; (C) NMT/chelidimerine, NMT/friedelin, and NMT/Hypericin. GP63, Glycoprotein 63; FPPS, farnesyl diphosphate synthase; NMT, N-myristoyltransferase.

RMSF

The RMSF quantifies the extent to which protein residues deviate from a reference location over time. The RMSF was used in these simulations to represent the residual movement of proteins away from the reference point during the simulation period. Three proteins of *L. major* showed no unintended fluctuations in the current simulation, demonstrating the stability of the interactions (Fig. 13).

The Rg analysis

Rg plot was used to assess the compactness of proteins. The results that are shown in Fig. 14 indicate the stability of the interactions of compounds with the key proteins of *L. major*. Eventually, the fluctuations become stable.

PCA

PCA may be a broadly utilized method for analyzing information from MD simulations of biomacromolecules. This might significantly reduce the size of their configuration space, accelerating future quantitative and qualitative inquiry. PCA examination of GP63/withaperuvin D, FPPS/strictinin, NMT/chelidimerine, NMT/friedelin, and NMT/hypericin interactions is illustrated in Fig. 15. In the binding of different ligands to NMT protein, the amount and patterns of folding were relatively similar.

H-bond

This plot displays the number of Hydrogen Bonds between the protein and the ligand during the simulation. In general, approximately 2, 4, 2, 1, and 2 h-bonds were observed for GP63/withaperuvin D, FPPS/strictinin, NMT/chelidimerine, NMT/friedelin, and NMT/hypericin, respectively (Fig. 16).

The SASA analysis

The surface of a protein that interacts with the solvent is called the SASA. Average SASA values for GP63/withaperuvin D, FPPS/strictinin, NMT/chelidimerine, NMT/friedelin, and NMT/hypericin complexes were monitored during 100 ns MD simulations. Figure 17 shows the SASA for the three proteins studied, GP63, FPPS, and NMT, indicating no major change in the SASA values between 50000 and 100000 ps. As a result, the graph confirms the stability of the interactions.

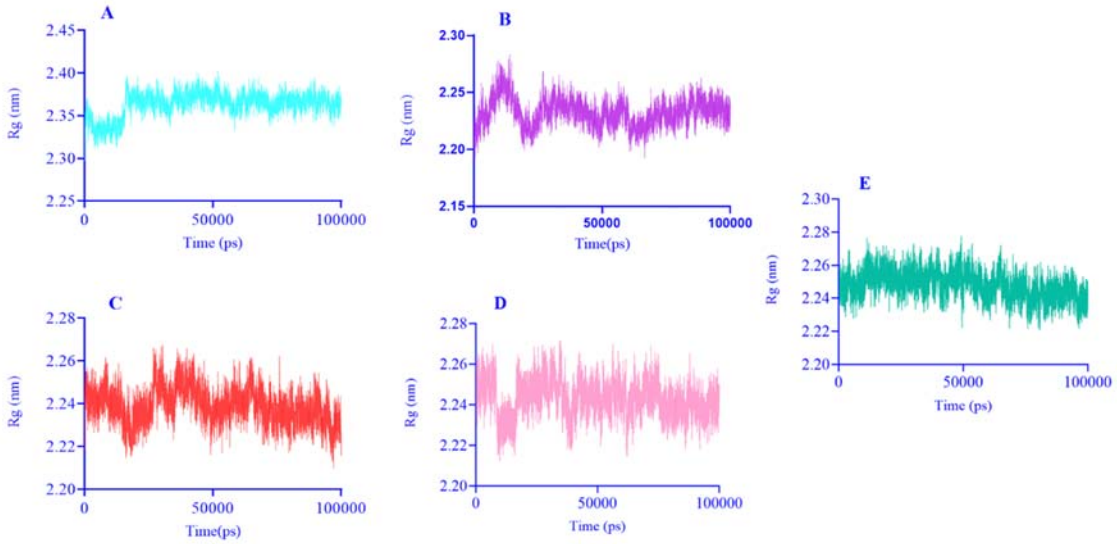

Fig. 14. The Rg diagrams of (A) GP63/withaperuvin D; (B) FPPS/strictinin; (C) NMT/chelidimerine; (D) NMT/friedelin; and (E) NMT/hypericin. Rg, Radius of gyration; GP63, glycoprotein 63; FPPS, farnesyl diphosphate synthase; NMT, N-myristoyltransferase.

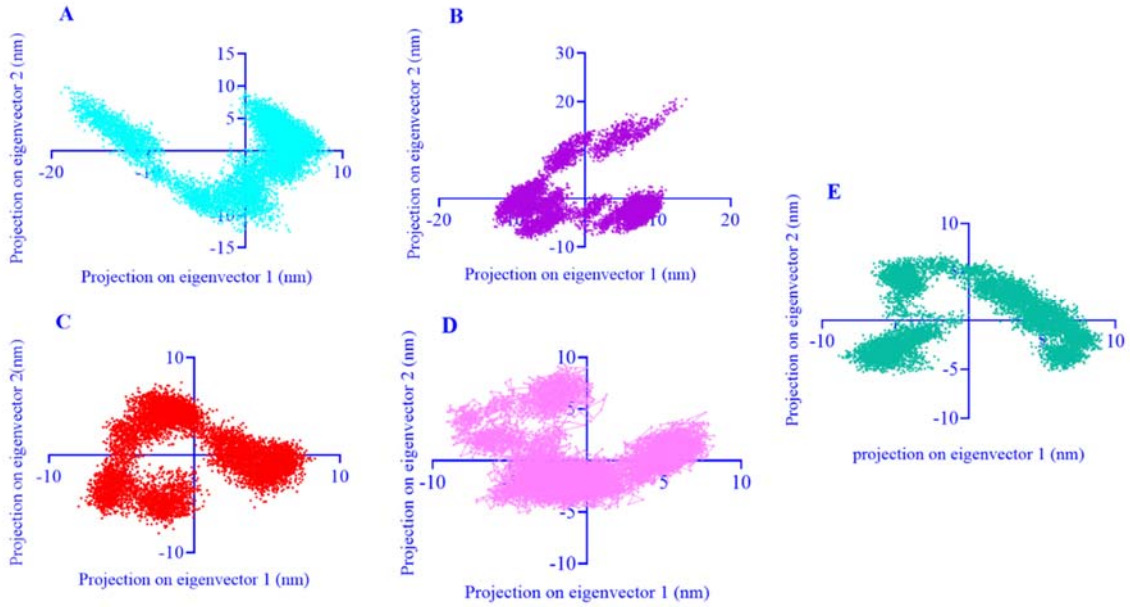

Fig. 15. Principal component analysis diagram of (A) GP63/withaperuvin D; (B) FPPS/strictinin; (C) NMT/chelidimerine; (D) NMT/friedelin; and (E) NMT/hypericin. GP63, glycoprotein 63; FPPS, farnesyl diphosphate synthase; NMT, N-myristoyltransferase.

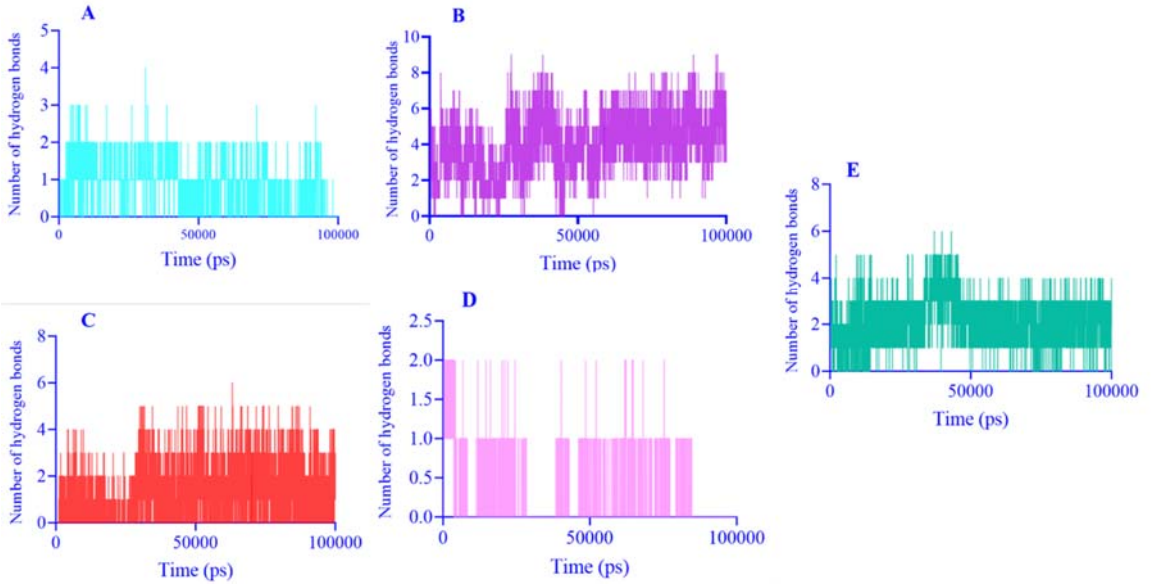

Fig. 16. The hydrogen bond diagrams of (A) GP63/withaperuvin D; (B) FPPS/strictinin; (C) NMT/chelidimerine; (D) NMT/friedelin; and (E) NMT/hypericin. GP63, glycoprotein 63; FPPS, farnesyl diphosphate synthase; NMT, N-myristoyltransferase.

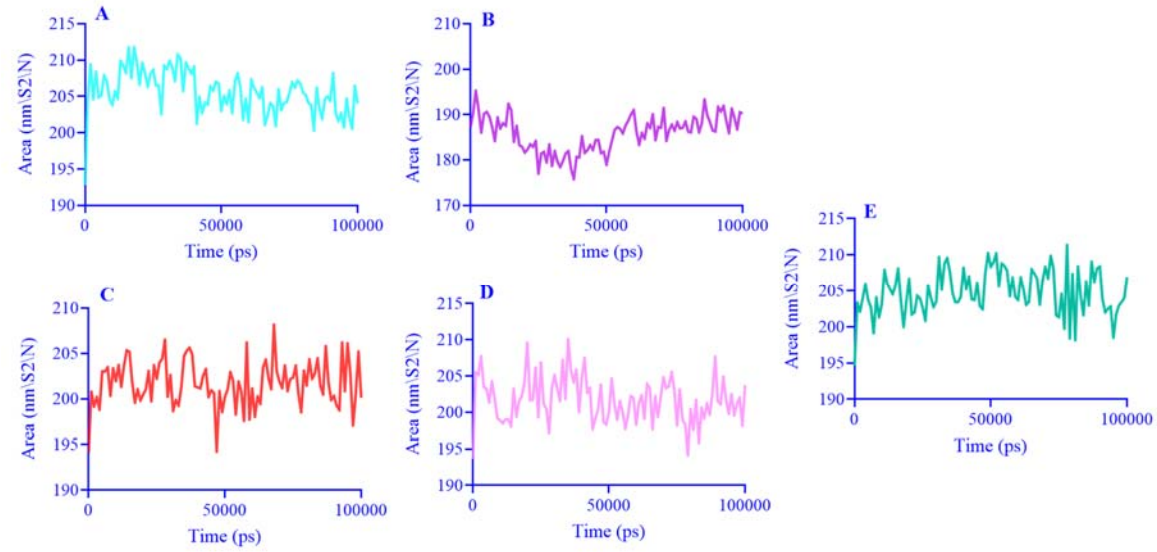

Fig. 17. The solvent accessible surface diagrams of (A) GP63/withaperuvin D; (B) FPPS/strictinin; (C) NMT/chelidimerine; (D) NMT/friedelin; and (E) NMT/hypericin. GP63, glycoprotein 63; FPPS, farnesyl diphosphate synthase; NMT, N-myristoyltransferase.

MMPBSA

The MMPBSA approach is frequently used for simulating free energy and modeling molecular recognition, such as protein-ligand interactions. The data and graphs showed that GP63/withaperuvin D interactions have a total binding energy of -18.11 (Fig. 18A), and FPPS/strictinin interactions have a total binding energy of -30.08 (Fig. 18B). In contrast to hypericin (Fig. 19C), which has a greater binding energy of roughly -37 in the interaction with NMT, two chemicals, chelidimerine and friedelin (Fig. 19A and B), had similar total binding energies.

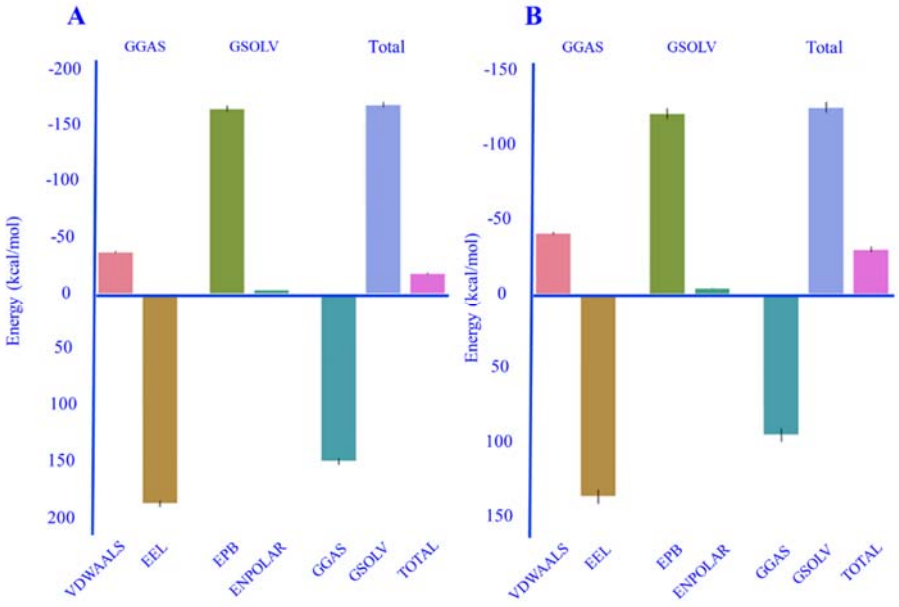

Fig. 18. The free energy of binding of (A) GP63/withaperuvin D and (B) FPPS/strictinin. GP63, glycoprotein 63; FPPS, farnesyl diphosphate synthase.

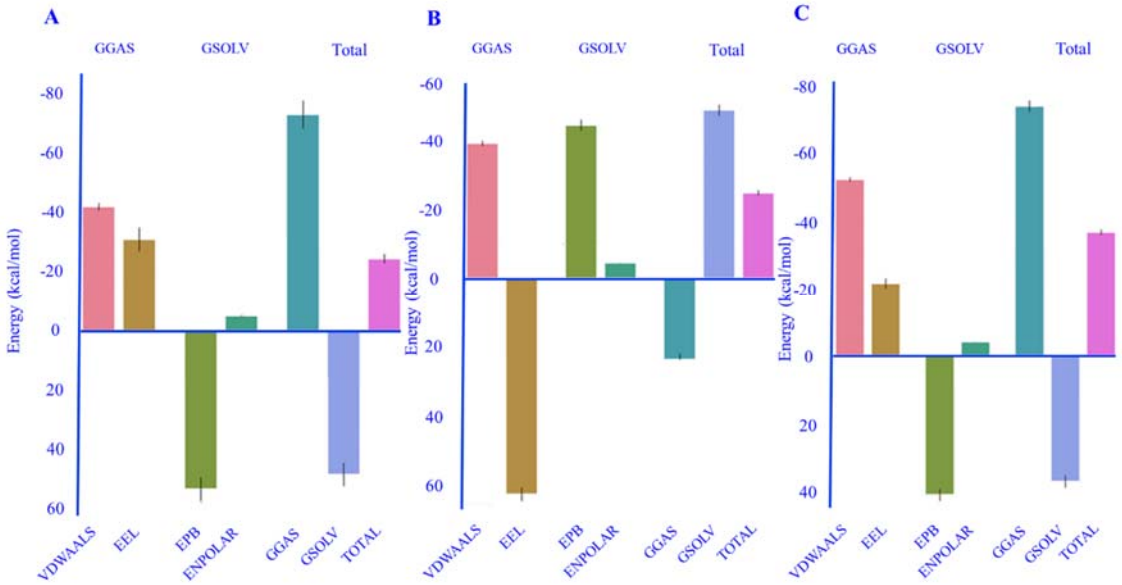

Fig. 19. The free energy of binding of (A) NMT/chelidimerine; (B) NMT/friedelin; and (C) NMT/hypericin. GP63, glycoprotein 63; FPPS, farnesyl diphosphate synthase; NMT, N-myristoyltransferase.

DISCUSSION

Four thousand active ingredients of medicinal plants were anchored on three important target proteins of *Leishmania* to find the best compounds to inhibit these proteins. Among them, 6 effective active ingredients with the highest affinity for proteins were obtained, including withaperuvin D, lagerstannin A, strictinin, chelidimerine, friedelin, and hypericin, and three amentoflavone, protohypericin, and luteolin 3'-o-glucuronide compounds, which had high binding affinity to all three NMT, FPPS, AND

GP63 proteins. According to previous studies that investigated several inhibitors of important *Leishmania* proteins, bisphosphonate, podocarpusflavone A, bipinnatone A, medicagenina, phenylbutazone, podocarpusflavone B, 3-fluoro-1-(2-hydroxy-2,2-diphosphonoethyl) pyridinium, piperidinylindole, amphotericin B, and thienopyrimidine have been introduced as the most common inhibitors of *Leishmania* proteins. The findings of molecular docking revealed that these compounds had a lower binding affinity than our suggested compounds, since the binding affinity and stability of the compounds in the current investigation were substantially greater than the examined blockers (49-52). Besides, the results showed that the current interactions are better than previous blockers because, unlike other blockers, many amino acids in the protein's active site are involved in the interaction and binding. Our proposed compounds can interact strongly and stably (ionic and covalent bonds) with the important amino acids of the active site of proteins, which deactivate their active site, and have a better binding score than common inhibitors, which improves the strength and stability of interactions. In the case of withaperuvin D, forming a suitable hydrogen bond between amino acids Ala225, Glu265, and His268 at the active site of GP63 protein requires the presence of different OH groups on the rings of this compound. Moreover, the presence of benzene and cycloalkane rings is fundamental for the hydrophobic interaction of pi-pi and pi-alkyl types with amino acids His268, Glu265, Val233, Ala348, and Ala349, and a docking score of -9.2 kcal/mol. In stable hydrogen interaction of strytinin with amino acids Asp250, Gly266, Ile265, Asp271, Thr106, Lys264, Ser104, Thr257, and Lys105 in the active site of FPPS protein, phenolic OH groups and oxygen play an important role. In addition, the benzene ring plays a role in the hydrophobic interaction with Asp271 and its docking score was about -10.1 kcal/mol. Furthermore, the hydrogen interaction between chylidimarin and the amino acids Asp396, Gly205, and His398 requires the presence of oxygen and nitrogen groups; this interaction had a docking score of -14.1 kcal/mol. Similarly, the hydrogen interaction between Friedlin and the amino acid Gly205 requires the presence of a carbonyl group; the docking score for this interaction was -12.7 kcal/mol. In hypericin, the presence of oxygen atoms in the structure of the compound in the form of carbonyl, and available to form a hydrogen bond with amino acids Tyr217, Phe168, Asn167, and Gly205, is necessary and its docking had a -12.5 kcal/mol score. Piperidinylindole has four hydrogen bonds with amino acids Thr193, Phe158, and Leu411. It has hydrophobic interactions with Gly195, Ala194, Val71, and Ieu159 amino acids. The desired compound had an electrostatic interaction of pi-sulfur, hydrophobic, and hydrogen type with the amino acid TYR70. The docking score of this compound with NMT was about -9.2 kcal/mol.

According to the results of MD (RMSD, RMSF, Rg, PCA, MMPBSA, and SASA), the surveyed interactions had little fluctuations from 50 ns onwards and the system had reached equilibrium. For example, as it is clear from the RMSF results, the amino acids Ala225, Glu265, His268, Val223, Leu224, which are important amino acids in the binding of GP63 to withaperuvin, are located in the 200-300 region of the diagram, which has the lowest energy and fluctuation. Also, regarding FPPS protein, amino acids Asp250, Gly266, Ile265, Lys264, Ser104, Thr257, Lys105, Thr106, Lys105, and Thr257 and NMT protein amino acids Tyr80, Phe88, Phe90, Val81, Val71, Leu399, Thr203, Thr70, Ala194, Gly195, His398, Asp396, and Gly205, which are the main amino acids in binding of compounds to proteins, showed the lowest fluctuation and energy level. Therefore, given the obtained results, the binding of the mentioned compounds to their proteins was stable. According to pharmaceutical databases such as Pass Online, chelidimerine, friedelin, amentoflavone, and luteolin 3'-o-glucuronide compounds have low side effects, antioxidant, anticancer, anti-inflammatory, anti-viral, anti-fungal, and anti-bacterial effects. They are anti-protozoal and strengthen the body's immune system and have wound-healing properties. In general, considering the high score of these compounds and the stability of MD results, it seems that these compounds are suitable for inhibiting the activity of *L. major* and they effectively inhibit the important proteins of the

parasite, and most likely, by inhibiting these proteins, they have a significant effect on inhibition of growth and reproduction of different stages of *Leishmania* parasite.

The six mentioned compounds are present as part of effective substances in the plants, such as *Plantago psyllium, Punica granatum, Juglans regia, Chelidonium majus, Albizia lebbeck, Cassia fistula*, and *Hypericum perforatum*, and three other compounds were obtained from *Hypericum perforatum, Trifolium pratense, Rosa canina, Glycyrrhiza glabra, Rhus coriaria*, and *Verbena officinalis* plants.

A significant disease in tropical and subtropical areas is leishmaniasis. The parasitic infection is caused by *Leishmania* parasites, which come in various kinds. The bite of a female sandfly carrying the parasites may transmit leishmaniasis (53). 350 million individuals are at risk of leishmaniasis, which is endemic in 98 nations (54). Infected people face many problems, including toxicity, extended treatment periods, expensive treatment costs, and a lack of an oral formulation. Therefore, creating novel medicines for the treatment of leishmaniasis is a global priority (55).

Based on the reports, the non-mutagenic and non-toxic substance hypericin may be able to cure cutaneous leishmaniasis based on photodynamic therapy (56) and target the parasite's spermidine synthase (57). Hypericin has been approved for use in humans by the FDA. Seplveda *et al.* found that in mice with leishmaniasis, TiO_2/Zn-hypericin-photodynamic therapy decreased the parasite load by 43% or 58% at dosages of 0.5 and 1.0 mg/kg/kg, respectively (58). After testing hypericin *in vitro* and *in vivo* on hamsters with cutaneous leishmaniasis (*L. panamensis*), Montoya *et al*. reported that hypericin's anti-amastigote actions decreased parasite burden and improved lesions (56).

The study conducted by Rizk *et al.* showed that amentoflavone had therapeutic benefits on the lesions and decreased the parasite burden in mice treated with *L. amazonensis*. They approved that the balance between anti-inflammatory and inflammatory patterns at the site of infection is significantly affected by amentoflavone (59, 60). Besides, amentoflavone was shown to have anticancer properties in a bioinformatics study (61). Additionally, a different *in-silico* study suggested that amentoflavone might block SARS-CoV-2 (62).

In studies on the amastigote state of leishmaniasis, the antileishmanial effect of plants containing friedelin has been observed as a reduction in the parasite burden (63, 64). Shi *et al.* investigated the effects of friedelin on ulcerative colitis in bioinformatics research carried out in 2021. They found that friedelin reduces ulcerative colitis *via* anti-inflammatory pathways and autophagy function (65). Strictinin treatment for hepatitis-infected mice cleared the viral infection. Stritinin probably prevents virus entrance and hinders crucial phases of viral infection (66).

The anti-leishmanial and anti-malarial activity of 32 medicinal plants, including *Rosmarinus officinalis*, was studied by Mothana and colleagues against the promastigotes of three different types of *Leishmania*, *L. tropica, L. infantum,* and *L. major*, *in vitro,* and they claimed that some species of the Lamiaceae family have antileishmania properties (23). The *in vitro* antileishmanial activity of several *Berberis vulgaris* extracts against promastigote and amastigote of *L. tropica* and *L. infantum* was evaluated in Mahmoudvand's work using a murine macrophage model. Moreover, they showed using the MTT assay that *B. vulgaris* possessed potent *in vitro* leishmanial activity against *L. tropica* and *L. infantum.* Compared to meglumine antimoniate, the growth rate of the promastigote stage of *L. tropicala* and *L. infantum* was significantly suppressed by *B. vulgaris,* specifically berberine, according to the results of optical density and IC_{50}. Furthermore, as compared to the positive control, *B. vulgaris* and berberine considerably reduced the mean number of amastigotes in each macrophage (67). *Tridax procumbens* extracts showed powerful effects in *in vitro* tests against the promastigotes form of *L. mexicana*, while having no side effects on mammalian cells. According to this study, there was a noticeable activity of tridax procumbens and (3S)-16,17-didehydrofalcarinol extracts against *L. mexicana*. With an IC_{50} of 3 µg/mL, the methanol extract suppressed the growth of

L. mexicana promastigotes, whereas oxylipin (3S)-16,17-didehydrofalcarinol showed the strongest inhibition at an IC_{50} of 0.478 µg/mL (68). *Urechites andrieuxii* (Apocynaceae) was tested for its *in vitro* antileishmanial activity, and an eye-catching result was obtained. The MTT test was used to evaluate the impact of the extract on the viability of parasites and cells derived from *Salvia verbenaca* (L.) Briq. ssp. verbenaca Maire (*S. clandestina* Batt. non L), which has previously shown antileishmanial activity *in vitro* (69). In an *in vitro* study done by Ezatpour *et al*. the results showed that the Anacardiaceae plant *Pistacia khinjuk* has antileishmanial activity against *L. tropica* and *L. major*. The extracts' anti-amastigote effect was assessed by counting the number of amastigotes in each macrophage and comparing the results to the positive control. The results of this investigation showed that *P. khinjuk* stimulated nitric oxide generation in comparison to untreated macrophages (70). In another *in vitro* research, the inhibitory effect of two extracts of the leaves of *Rhazya stricta* and *Calotropis procera* plants on both the amastigote and promastigote stages of *L. major* was reported (71). The fruit extract and its components from *Citrullus colocyn* demonstrated antileishmanial activities. A study investigating the impact of several essential oils derived from different plants on *L. amazonensis* promastigotes found that although the essential oils had little cytotoxic effect on L6 cells, they were successful in combating *L. amazonensis* promastigotes (72). In another study, MTT measurements were used to evaluate the antileishmanial impact of *Artemisia sieberi's* essential oil on *L. infantum*. However, numerous *in vitro* studies showed that a variety of plants have powerful antileishmanial properties (73).

L. major can be treated well with *Plantago psyllium* alone and in conjunction with white vinegar, according to studies (74). In 2020, Mardani *et al*. found that the ethanolic extract of *Punica granatum*'s fruit peel had a much higher anti-*L. major* action than the ethanolic extract of the plant's flower (75). Based on the bioinformatics studies, *Withania somnifera*'s leaves, roots, and fruits possess powerful antiprotozoal compounds that are effective against *Trypanosoma*, *Plasmodum*, and *Leishmania* species and demonstrate their antileishmanial role by NMT inhibition (31). Because *Chrysanthemum morifolium* includes potent substances, including luteolin and phenolic compounds, previous studies have shown that it possesses antioxidant, anticancer, anti-inflammatory, antifungal, antileishmanial, and antiviral effects (38, 75, 76). An aqueous extract of *Juglans regia* root was found to have antibacterial, insecticidal, and antileishmanial (*L. amazonensis*) properties in an *in vitro* and *in silico* study (77). According to a study by Ashoori *et al*., the hydroalcoholic extract of *Rhus coriaria* fruits inhibits the growth of both promastigote and amastigote forms of *L. major* (78). In research, the effect of *Perovskia abrotanoides* extract on *Trypanosoma*, *Leishmania,* and *Plasmodium* was investigated, and among the effective substances of this plant, carnosol had a high inhibitory effect on these parasites (36). Iqbal *et al*. reported the anti-*L. tropica* effect of *Lawsonia inermis* extract in an in vitro study (37).

Ulger *et al.* reported the anti-*L tropica* effect of *Hypericum perforatum* leaf extract due to the presence of hypericin (79). The findings demonstrated that *Hypericum perforatum* contains various useful chemicals that exhibit a strong interaction with the three *L. major* proteins chosen in this technique, in addition to the two common compounds amentoflavone and protohypericin (picked in the current research). Besides, the plants, such as *Rhus coriaria, Trifolium pratense, Rosa canina, Glycyrrhiza glabra, and Chrysanthemum morifolium,* contain several desired compounds. Considering the activity of these compounds, including antioxidant, anti-inflammatory, anti-protozoal (*Leishmania*), anti-infective, anti-parasitic, anti-psoriatic, anti-viral, anti-eczematic, and immune system stimulant related to the treatment of leishmaniasis, there is a possibility that the plant containing them also shows the same inhibitory effect. The same effects help to heal wounds and treat *leishmaniasis*.

According to Tasdemir *et al*.'s study on the antitrypanosomal and antileishmanial activities of flavonoids and their analogues, flavone luteolin was one of the most effective

compounds in inhibiting *L. donovani*, with an IC_{50} of 0.8 µg/mL. This finding is consistent with the findings of flavones, anthroquinons, withanolide, isoquinolins, *etc*. Its IC_{50} was about the same as miltefosine, an antileishmanial drug used in clinics (IC_{50} of 0.34 g/mL).. The benzo-chromone component of the flavone structure was not significantly altered by the addition of a single OH group, but the leishmanicidal potential was significantly enhanced by the addition of two OH functionalities. Important roles were C-5, C-7, and C-8. Although ring B's hydroxylation had a considerable effect on the activity, a distinct SAR could not be seen. For instance, luteolin, which has a catechol (3,4-dihydroxyphenyl) moiety and a 5,7-dihydroxybenzochromone structure, has an IC_{50} of 0.8 g/mL, which is twice as effective as apigenin's (IC_{50} of 1.9 g/mL), which has a p-hydroxyphenyl side chain. Luteolin showed the greatest combination by having four OH groups at the C-5, C-7, C-3', and C-4' positions (80).

The investigations of previous articles revealed that no bioinformatic studies, especially related to leishmaniasis, were performed on these compounds, and only amentoflavone, friedelin, and hypericin were clinically investigated. Therefore, most of these compounds were proposed for the first time in this study. Furthermore, most of the plants that contain these compounds were not studied for leishmaniasis, especially *L. major*, or the compounds and their mechanisms of action on parasites and disease were not studied in detail. The present study identified which essential *L. major* protein may be suppressed by which potent herbal remedy, and to what degree leishmaniasis can be treated and prevented by avoiding the emergence of which stages of the illness. However, more experimental research and clinical trial tests on these proposed compounds and plants are needed to make sure of their antileishmanial effects.

CONCLUSION

Based on the study, effective substances withaperuvin D, lagerstannin A, strictinin, chelidimerine, friedelin, hypericin, amentoflavone, protohypericin, and luteolin 3'-o-glucuronide had the greatest binding affinity for vital proteins of *Leishmania* GP63, FPPS, and NMT. Furthermore, the examination of the aforementioned drug databases revealed that none of them exhibited adverse effects. Furthermore, they potentially possessed properties such as wound healing, immune system enhancement, antioxidant, anticarcinogenic, anti-inflammatory, antiviral, antineoplastic, antifungal, and antimicrobial activity. Consequently, plants containing these substances, especially those with one or more compounds amentoflavone, protohypericin, and luteolin 3'-o-glucuronide, are suggested for the effective treatment of *L. major*. So, these compounds could be an effective treatment for leishmaniasis. To ensure their antileishmanial effects on the *L. major* parasite, further clinical studies are required.

Acknowledgments

The authors are thankful to the National Institute of Genetic Engineering and Biotechnology (NIGEB) for their support and facilities. The present study was extracted from a Ph.D. dissertation in the Department of Mycology and Parasitology, School of Medicine, Isfahan University of Medical Sciences, Isfahan, Iran, which was financially supported by the Vice-Chancellery for Research and Technology, Isfahan University of Medical Sciences, Isfahan, Iran, through Grant No. 3400997.

Conflicts of interest statement

The authors declared no conflict of interest in this study.

Authors' contributions

All authors equally contributed to this work, outlined the manuscript, and critically revised it. The finalized article was read and approved by all authors.

REFERENCES

1. Olivier M, Hassani K. Protease inhibitors as prophylaxis against leishmaniasis: new hope from the major surface protease gp63. Future Med Chem. 2010;2(4):539-542.
DOI: 10.4155/fmc.10.17.

2. Sheikhmoradi V, Saberi S, Saghaei L, Pestehchian N, Fassihi A. Synthesis and antileishmanial activity of antimony (V) complexes of hydroxypyranone and hydroxypyridinone ligands. Res Pharm Sci. 2018;13(2):111-120. DOI: 10.4103/1735-5362.223793.
3. Rahnama V, Motazedian MH, Mohammadi-Samani S, Asgari Q, Ghasemiyeh P, Khazaei M. Artemether-loaded nanostructured lipid carriers: preparation, characterization, and evaluation of *in vitro* effect on *Leishmania major*. Res Pharm Sci. 2021;16(6):623-633. DOI: 10.4103/1735-5362.327508.
4. Joshi PB, Kelly BL, Kamhawi S, Sacks DL, McMaster WR. Targeted gene deletion in Leishmania major identifies leishmanolysin (GP63) as a virulence factor. Mol Biochem Parasitol. 2002;120(1): 33-40. DOI: 10.1016/s0166-6851(01)00432-7.
5. Bowyer PW, Gunaratne RS, Grainger M, Withers-Martinez C, Wickramsinghe SR, Tate EW, *et al*. Molecules incorporating a benzothiazole core scaffold inhibit the N-myristoyltransferase of *Plasmodium falciparum*. Biochem J. 2007;408(2):173-180. DOI: 10.1042/bj20070692.
6. Rogers MJ, Mönkkönen J, Munoz MA. Molecular mechanisms of action of bisphosphonates and new insights into their effects outside the skeleton. Bone. 2020;139:115493,1-39. DOI: 10.1016/j.bone.2020.115493.
7. Mukherjee S, Basu S, Zhang K. Farnesyl pyrophosphate synthase is essential for the promastigote and amastigote stages in *Leishmania major*. Mol Biochem Parasitol. 2019;230:8-15. DOI: 10.1016/j.molbiopara.2019.03.001.
8. Sanders JM, Song Y, Chan JMW, Zhang Y, Jennings S, Kosztowski T, *et al*. Pyridinium-1-yl bisphosphonates are potent inhibitors of farnesyl diphosphate synthase and bone resorption. J Med Chem. 2005;48(8):2957-2963. DOI: 10.1021/jm040209d.
9. Brannigan JA, Roberts SM, Bell AS, Hutton JA, Hodgkinson MR, Tate EW, *et al*. Diverse modes of binding in structures of *Leishmania major* N-myristoyltransferase with selective inhibitors. IUCrJ. 2014;1(4):250-260. DOI: 10.1107/S2052252514013001.
10. Frearson JA, Brand S, McElroy SP, Cleghorn LA, Smid O, Stojanovski L, *et al*. N-myristoyltransferase inhibitors as new leads to treat sleeping sickness. Nature. 2010;464(7289):728-732. DOI: 10.1038/nature08893.
11. Kim JH, Didi-Cohen S, Khozin-Goldberg I, Zilberg D. Translating the diatom-grazer defense mechanism to antiparasitic treatment for monogenean infection in guppies. Algal Res. 2021;58:102426. DOI: 10.1016/j.algal.2021.102426.
12. Wright MH, Paape D, Storck EM, Serwa RA, Smith DF, Tate EW. Global analysis of protein N-myristoylation and exploration of N-myristoyltransferase as a drug target in the neglected human pathogen *Leishmania donovani*. Chem Biol. 2015;22(3):342-354. DOI: 10.1016/j.chembiol.2015.01.003.
13. Price HP, Güther MLS, Ferguson MA, Smith DF. Myristoyl-CoA: protein N-myristoyltransferase depletion in trypanosomes causes avirulence and endocytic defects. Mol Biochem Parasitol. 2010;169(1):55-58. DOI: 10.1016/j.molbiopara.2009.09.006.
14. Price HP, Menon MR, Panethymitaki C, Goulding D, McKean PG, Smith DF. Myristoyl-CoA: protein N-myristoyltransferase, an essential enzyme and potential drug target in kinetoplastid parasites. J Biol Chem. 2003;278(9):7206-7214. DOI: 10.1074/jbc.M211391200.
15. Grogl M, Thomason TN, Franke ED. Drug resistance in leishmaniasis: its implication in systemic chemotherapy of cutaneous and mucocutaneous disease. Am J Trop Med Hyg. 1992;47(1):117-126. DOI: 10.4269/ajtmh.1992.47.117.
16. Olías-Molero AI, de la Fuente C, Cuquerella M, Torrado JJ, Alunda JM. Antileishmanial drug discovery and development: time to reset the model? Microorganisms. 2021;9(12):2500,1-18. DOI: 10.3390/microorganisms9122500.
17. Schlagenhauf E, Etges R, Metcalf P. The crystal structure of the *Leishmania major* surface proteinase leishmanolysin (gp63). Structure. 1998;6(8):1035-1046. DOI: 10.1016/s0969-2126(98)00104-x.
18. Ferreira GE, dos Santos BN, Dorval ME, Ramos TP, Porrozzi R, Peixoto AA, *et al*. The genetic structure of *Leishmania infantum* populations in Brazil and its possible association with the transmission cycle of visceral leishmaniasis. PloS One. 2012;7(5):e36242,1-10. DOI: 10.1371/journal.pone.0036242.
19. Ferrer-Casal M, Li C, Galizzi M, Stortz CA, Szajnman SH, Docampo R, *et al*. New insights into molecular recognition of 1,1-bisphosphonic acids by farnesyl diphosphate synthase. Bioorg Med Chem. 2014;22(1):398-405. DOI: 10.1016/j.bmc.2013.11.010.
20. Källberg M, Wang H, Wang S, Peng J, Wang Z, Lu H, *et al*. Template-based protein structure modeling using the RaptorX web server. Nat Protoc. 2012;7(8):1511-1522. DOI: 10.1038/nprot.2012.085.
21. Kim S, Chen J, Cheng T, Gindulyte A, He J, He S, *et al*. PubChem 2019 update: improved access to chemical data. Nucleic Acids Res. 2019;47(D1):D1102-D1109. DOI: 10.1093/nar/gky1033.
22. Yildirim A, Mavi A, Oktay M, Kara AA, Algur OF, Bilaloglu V. Comparison of antioxidant and antimicrobial activities of tilia (*Tilia argentea* Desf ex DC), sage (*Salvia triloba* L.), and black tea (*Camellia sinensis*) extracts. J Agric Food Chem. 2000;48(10):5030-5034. DOI: 10.1021/jf000590k.
23. Mothana RA, Al-Musayeib NM, Al-Ajmi MF, Cos P, Maes L. Evaluation of the *in vitro* antiplasmodial,

antileishmanial, and antitrypanosomal activity of medicinal plants used in Saudi and Yemeni traditional medicine. Evid Based Complement Alternat Med. 2014;2014:905639,1-8.
DOI: 10.1155/2014/905639.
24. Berman HM, Westbrook J, Feng Z, Gilliland G, Bhat TN, Weissig H, *et al*. The protein data bank. Nucleic Acids Res. 2000;28(1):235-242.
DOI: 10.1093/nar/28.1.235.
25. Shaukat A, Mirza H, Ansari A, Yasinzai M, Zaidi S, Dilshad S, *et al*. Benzimidazole derivatives: synthesis, leishmanicidal effectiveness, and molecular docking studies. Med Chem Res. 2012;22:3606-3620.
DOI: 10.1007/s00044-012-0375-5.
26. Mercado-Camargo J, Cervantes-Ceballos L, Vivas-Reyes R, Pedretti A, Serrano-García ML, Gómez-Estrada H. Homology modeling of leishmanolysin (gp63) from *Leishmania panamensis* and molecular docking of flavonoids. ACS Omega. 2020;5(24):14741-14749.
DOI: 10.1021/acsomega.0c01584.
27. Aripirala S, Gonzalez-Pacanowska D, Oldfield E, Kaiser M, Amzel LM, Gabelli SB. Structural and thermodynamic basis of the inhibition of *Leishmania major* farnesyl diphosphate synthase by nitrogen-containing bisphosphonates. Acta Crystallogr D Biol Crystallogr. 2014;70(Pt 3):802-810.
DOI: 10.1107/s1399004713033221.
28. de Mattos Oliveira L, Araújo JSC, Bacelar Costa Junior D, Santana IB, Duarte AA, Leite FHA, *et al*. Pharmacophore modeling, docking and molecular dynamics to identify *Leishmania major* farnesyl pyrophosphate synthase inhibitors. J Mol Model. 2018;24(11):314,1-12.
DOI: 10.1007/s00894-018-3838-x.
29. Gadelha APR, Brigagao CM, da Silva MB, Rodrigues ABM, Guimarães ACR, Paiva F, *et al*. Insights about the structure of farnesyl diphosphate synthase (FPPS) and the activity of bisphosphonates on the proliferation and ultrastructure of *Leishmania* and *Giardia*. Parasit Vectors. 2020;13(1):168,1-18.
DOI: 10.1186/s13071-020-04019-z.
30. Brannigan JA, Smith BA, Yu Z, Brzozowski AM, Hodgkinson MR, Maroof A, *et al*. N-myristoyltransferase from *Leishmania donovani*: structural and functional characterisation of a potential drug target for visceral leishmaniasis. J Mol Biol. 2010;396(4):985-999.
DOI: 10.1016/j.jmb.2009.12.032.
31. Orabi MAA, Alshahrani MM, Sayed AM, Abouelela ME, Shaaban KA, Abdel-Sattar ES. Identification of potential leishmania N-myristoyltransferase inhibitors from *Withania somnifera* (L.) Dunal: a molecular docking and molecular dynamics investigation. Metabolites. 2023;13(1):93,1-25.
DOI: 10.3390/metabo13010093.
32. Hussein NN, Al-Azawi K, Sulaiman GM, Albukhaty S, Al-Majeed RM, Jabir M, *et al*. Silver-cored *Ziziphus spina-christi* extract-loaded antimicrobial nanosuspension: overcoming multidrug resistance. Nanomedicine (Lond). 2023;18(25):1839-1854.
DOI: 10.2217/nnm-2023-0185.
33. Anyanwu MU, Okoye RC. Antimicrobial activity of Nigerian medicinal plants. J Intercult Ethnopharmacol. 2017;6(2):240-259.
DOI: 10.5455/jice.20170106073231.
34. Duraipandiyan V, Ayyanar M, Ignacimuthu S. Antimicrobial activity of some ethnomedicinal plants used by Paliyar tribe from Tamil Nadu, India. BMC Complement Altern Med. 2006;6:35,1-7.
DOI: 10.1186/1472-6882-6-35
35. Ertürk Ö. Antibacterial and antifungal effects of alcoholic extracts of 41 medicinal plants growing in Turkey. Czech J. Food Sci. 2010;28(1):53-60.
DOI: 10.17221/144/2008-CJFS.
36. Tabefam M, Farimani MM, Danton O, Ramseyer J, Kaiser M, Ebrahimi SN, *et al*. Antiprotozoal diterpenes from *Perovskia abrotanoides*. Planta Med. 2018;84(12-13):913-919.
DOI: 10.1055/a-0608-4946.
37. Iqbal K, Iqbal J, Staerk D, Kongstad KT. Characterization of antileishmanial compounds from *Lawsonia inermis* L. leaves using semi-high resolution antileishmanial profiling combined with HPLC-HRMS-SPE-NMR. Front Pharmacol. 2017;8:337,1-7.
DOI: 10.3389/fphar.2017.00337.
38. Zhan J, He F, Cai H, Wu M, Xiao Y, Xiang F, *et al*. Composition and antifungal mechanism of essential oil from *Chrysanthemum morifolium* cv. Fubaiju. J Funct Foods. 2021;87:104746,1-8.
DOI: 10.1016/j.jff.2021.104746.
39. Kim S, Thiessen PA, Bolton EE, Chen J, Fu G, Gindulyte A, *et al*. PubChem substance and compound databases. Nucleic Acids Res. 2016;44(D1):D1202-D1213.
DOI: 10.1093/nar/gkv951.
40. Pettersen EF, Goddard TD, Huang CC, Couch GS, Greenblatt DM, Meng EC, *et al*. UCSF chimera-a visualization system for exploratory research and analysis. J Comput Chem. 2004;25(13):1605-1612.
DOI: 10.1002/jcc.20084.
41. Shravani S. Pawar SHR. Review on discovery studio: an important tool for molecular docking. Asian J Research Chem. 2021;14(1):86-88.
DOI: 10.5958/0974-4150.2021.00014.6.
42. Poroikov VV, Filimonov DA, Gloriozova TA, Lagunin AA, Druzhilovskiy DS, Rudik AV, *et al*. Computer-aided prediction of biological activity spectra for organic compounds: the possibilities and limitations. Russ Chem Bull. 2019;68(12):2143-2154.
DOI: 10.1007/s11172-019-2683-0.
43. Maunz A, Gütlein M, Rautenberg M, Vorgrimmler D, Gebele D, Helma C. lazar: a modular predictive toxicology framework. Front Pharmacol. 2013;4:38,1-10.
DOI: 10.3389/fphar.2013.00038.
44. Daina A, Michielin O, Zoete V. SwissADME: a free web tool to evaluate pharmacokinetics, drug-likeness and medicinal chemistry friendliness of small molecules. Sci Rep. 2017;7(1):42717,1-13.
DOI: 10.1038/srep42717.

45. Abraham MJ, Murtola T, Schulz R, Páll S, Smith JC, Hess B, *et al*. GROMACS: high performance molecular simulations through multi-level parallelism from laptops to supercomputers. SoftwareX. 2015;1-2:19-25. DOI: 10.1016/j.softx.2015.06.001
46. Alimardan Z, Abbasi M, Khodarahmi G, Kashfi K, Hasanzadeh F, Mahmud A. Identification of new small molecules as dual FoxM1 and Hsp70 inhibitors using computational methods. Res Pharm Sci. 2022;17(6):635-656. DOI: 10.4103/1735-5362.359431.
47. Valdés-Tresanco MS, Valdés-Tresanco ME, Valiente PA, Moreno E. gmx_MMPBSA: a new tool to perform end-state free energy calculations with GROMACS. J Chem Theory Comput. 2021;17(10):6281-6291. DOI: 10.1021/acs.jctc.1c00645.
48. Luckman SP, Hughes DE, Coxon FP, Graham R, Russell G, Rogers MJ. Nitrogen-containing bisphosphonates inhibit the mevalonate pathway and prevent post-translational prenylation of GTP-binding proteins, including Ras. J Bone Miner Res. 1998;13(4):581-589. DOI: 10.1359/jbmr.1998.13.4.581.
49. Torres-Santos E, Lopes D, Oliveira R, Carauta JPP, Falcao C, Kaplan MAC, *et al*. Antileishmanial activity of isolated triterpenoids from *Pourouma guianensis*. Phytomedicine. 2004;11(2-3):114-120. DOI: 10.1078/0944-7113-00381.
50. Mesa C, Blandón G, Muñoz D, Muskus C, Florez A, Ochoa R, *et al*. *In silico* screening of potential drug with antileishmanial activity and validation of their activity by *in vitro* and *in vivo* studies. J Chem Chem Eng. 2015;9:375-402. DOI: 10.17265/1934-7375/2015.06.002.
51. Mojallal-Tabatabaei Z, Foroumadi P, Toolabi M, Goli F, Moghimi S, Kaboudanian-Ardestani S, *et al*. 2-(Bipiperidin-1-yl)-5-(nitroaryl)-1,3,4-thiadiazoles: synthesis, evaluation of *in vitro* leishmanicidal activity, and mechanism of action. Bioorg Med Chem. 2019;27(16):3682-3691. DOI: 10.1016/j.bmc.2019.07.009.
52. Qureshi KA, Al Nasr I, Koko WS, Khan TA, Fatmi MQ, Imtiaz M, *et al*. *In vitro* and *in silico* approaches for the antileishmanial activity evaluations of actinomycins isolated from novel *Streptomyces smyrnaeus* strain UKAQ_23. Antibiotics (Basel). 2021;10(8),887,1-17. DOI: 10.3390/antibiotics10080887.
53. Badirzadeh A, Taheri T, Taslimi Y, Abdossamadi Z, Heidari-Kharaji M, Gholami E, *et al*. Arginase activity in pathogenic and non-pathogenic species of *Leishmania* parasites. PLoS Negl Trop Dis. 2017;11(7):e0005774,1-22. DOI: 10.1371/journal.pntd.0005774.
54. Heidari-Kharaji M, Badirzadeh A, Khadir F, Soori M. Herbal drugs with promising anti-leishmanial activity: new hope for leishmaniasis treatment. J Skin Stem Cell. 2016;3(2):e66527. DOI: 10.5812/jssc.66527.
55. Miguel DC, Yokoyama-Yasunaka JK, Uliana SR. Tamoxifen is effective in the treatment of *Leishmania amazonensis* infections in mice. PLoS Negl Trop Dis. 2008;2(6):e249,1-5. DOI: 10.1371/journal.pntd.0000249.
56. Montoya A, Daza A, Muñoz D, Ríos K, Taylor V, Cedeño D, *et al*. Development of a novel formulation with hypericin to treat cutaneous leishmaniasis based on photodynamic therapy in *in vitro* and *in vivo* studies. Antimicrob Agents Chemother. 2015;59(9):5804-5813. DOI: 10.1128/aac.00545-15.
57. Singh S, Sarma S, Katiyar SP, Das M, Bhardwaj R, Sundar D, *et al*. Probing the molecular mechanism of hypericin-induced parasite death provides insight into the role of spermidine beyond redox metabolism in *Leishmania donovani*. Antimicrob Agents Chemother. 2015;59(1):15-24. DOI: 10.1128/aac.04169-14.
58. Sepúlveda AAL, Arenas Velásquez AM, Patiño Linares IA, de Almeida L, Fontana CR, Garcia C, *et al*. Efficacy of photodynamic therapy using TiO2 nanoparticles doped with Zn and hypericin in the treatment of cutaneous Leishmaniasis caused by *Leishmania amazonensis*. Photodiagnosis Photodyn Ther. 2020;30:101676. DOI: 10.1016/j.pdpdt.2020.101676.
59. Rizk YS, Santos-Pereira S, Gervazoni L, Hardoim DJ, Cardoso FO, de Souza C, *et al*. Amentoflavone as an ally in the treatment of cutaneous Leishmaniasis: analysis of its antioxidant/prooxidant mechanisms. Front Cell Infect Microbiol. 2021;11:615814,1-13. DOI: 10.3389/fcimb.2021.615814.
60. Rizk YS, Hardoim DdJ, Santos KBA, Zaverucha-do-Valle T, Taniwaki NN, Almeida-Souza F, *et al*. Amentoflavone isolated from *Selaginella sellowii* Hieron induces mitochondrial dysfunction in *Leishmania amazonensis* promastigotes. Parasitol Int. 2022;86:102458. DOI: 10.1016/j.parint.2021.102458.
61. Chen L, Fang B, Qiao L, Zheng Y. Discovery of anticancer activity of amentoflavone on esophageal squamous cell carcinoma: bioinformatics, structure-based virtual screening, and biological evaluation. J Microbiol Biotechnol. 2022;32(6):718-729. DOI: 10.4014/jmb.2203.03050.
62. Hossain R, Mahmud S, Khalipha ABR, Saikat ASM, Dey D, Khan RA, *et al*. Amentoflavone derivatives against SARS-CoV-2 main protease (M PRO): an *in silico* study. Main Group Chem. 2023;22:313-327. DOI: 10.3233/MGC-220077.
63. Garcia AR, Amaral ACF, Azevedo MMB, Corte-Real S, Lopes RC, Alviano CS, *et al*. Cytotoxicity and anti-Leishmania amazonensis activity of *Citrus sinensis* leaf extracts. Pharm Biol. 2017;55(1):1780-1486. DOI: 10.1080/13880209.2017.1325380.
64. Macedo SRA, Ferreira AS, de Barros NB, de Oliveira Meneguetti DU, Facundo VA, Shibayama TY, *et al*. Evaluation of the antileishmanial activity of biodegradable microparticles containing a hexanic eluate subfraction of *Maytenus guianensis* bark. Exp Parasitol. 2019;205:107738. DOI: 10.1016/j.exppara.2019.107738.

65. Shi B, Liu S, Huang A, Zhou M, Sun B, Cao H, *et al*. Revealing the mechanism of Friedelin in the treatment of ulcerative colitis based on network pharmacology and experimental verification. Evid Based Complement Alternat Med. 2021;2021:4451779,1-14. DOI: 10.1155/2021/4451779.
66. Tu E-C, Hsu W-L, Tzen JTC. Strictinin, a major ingredient in Yunnan Kucha tea possessing inhibitory activity on the infection of mouse hepatitis virus to mouse L cells. Molecules. 2023;28(3):1080,1-15. DOI: 10.3390/molecules28031080.
67. Mahmoudvand H, Sharififar F, Sharifi I, Ezatpour B, Fasihi Harandi M, Makki MS, *et al*. *In vitro* inhibitory effect of *Berberis vulgaris* (Berberidaceae) and its main component, berberine against different *Leishmania* species. Iran J Parasitol. 2014;9(1):28-36. PMID: 25642257.
68. Martín-Quintal Z, Moo-Puc R, González-Salazar F, Chan-Bacab MJ, Torres-Tapia LW, Peraza-Sánchez SR. *In vitro* activity of *Tridax procumbens* against promastigotes of *Leishmania mexicana*. J Ethnopharmacol. 2009;122(3):463-467. DOI: 10.1016/j.jep.2009.01.037.
69. Et-Touys A, Fellah H, Sebti F, Mniouil M, Aneb Mh, Elboury H, *et al*. In vitro antileishmanial activity of extracts from endemic Moroccan medicinal plant *Salvia verbenaca* (L.) Briq. ssp verbenaca Maire (*S. clandestina* Batt. non L). Eur J Med Plant. 2016;16(1):1-8. DOI: 10.9734/EJMP/2016/27891.
70. Ezatpour B, Saedi Dezaki E, Mahmoudvand H, Azadpour M, Ezzatkhah F. In vitro and *in vivo* antileishmanial effects of *Pistacia khinjuk* against *Leishmania tropica* and *Leishmania major.* Evid Based Complement Alternat Med. 2015;2015:149707,1-6. DOI: 10.1155/2015/149707.
71. Al Nasr IS. Evaluation of the *in vitro* antileishmanial activities of bioactive guided fractionations of two medicinal plants. Trop Biomed. 2020;37(1):15-23. PMID: 33612714.
72. Andrade MA, Azevedo CD, Motta FN, Santos ML, Silva CL, Santana JM, *et al*. Essential oils: *in vitro* activity against *Leishmania amazonensis*, cytotoxicity and chemical composition. BMC Complement Altern Med. 2016;16(1):444,1-8. DOI: 10.1186/s12906-016-1401-9
73. Tabari MA, Youssefi MR, Moghaddas E, Ebrahimi MA, Mousavi NN, Naseri A. Antileishmanial activity of *Artemisia sieberi* essential oil against *Leishmania infantum in vitro*. Adv Herb Med. 2017;3(2):40-46.
74. Moshfe A, Karami K, Bahmani M, Naghmachi M, Askarian S, Rezaei A, *et al*. Anti leishmanial effect of *Plantago psyllium* (Ovate) and white vinegar on *Leishmania major* lesion in BALB/c mice. Iran J Arthropod Borne Dis. 2022;16(1):45-50. DOI: 10.18502/jad.v16i1.11191.
75. Mardani H, Khalili B, Saberi S, Lorogooini Z, Ghaderi M, Abdizadeh R. Effect of hydroalcoholic extracts of flower and fruit peel of *Punica granatum* on *Leishmania major* promastigotes *in vitro*. Adv Herb Med. 2020;6:32-48
76. Li Y, Hao Y, Gao B, Geng P, Huang H, Yu L, *et al*. Chemical profile and *in vitro* gut microbiota modulatory, anti-inflammatory and free radical scavenging properties of *Chrysanthemum morifolium* cv. Fubaiju. J Funct Foods. 2019;58:114-122. DOI: 10.1016/j.jff.2019.04.053.
77. Ellafi A, Farhat R, Snoussi M, Noumi E, Anouar EH, Ben Ali R, *et al*. Phytochemical profiling, antimicrobial, antibiofilm, insecticidal, and anti-leishmanial properties of aqueous extract from *Juglans regia* L. root bark: *in vitro* and *in silico* approaches. Int J Food Prop. 2023;26(1):1079-1097. DOI: 10.1080/10942912.2023.2200561.
78. Ashoori F, Fakhar M, Goli HR, Mirzaee F, Faridnia R, Kalani H, *et al*. Antileishmanial and antibacterial activities of the hydroalcoholic extract of *Rhus coriaria* L. Ann Parasitol. 2020;62(2): 157-163. DOI: 10.17420/ap6602.250.
79. ÜLger ST, DelİAlİOĞLu N, GÜLtekİN EO, Aslan G, Yabalak E, ÜLger M, *et al*. *In vitro* antileishmanial effect of the plant extracts from *Aloe vera* (L.) Burm.f. and hypericum perforatum l. leaves. Kafkas Univ Vet Fak Derg. 2021;27(3):363-370. DOI: 10.9775/kvfd.2021.25633.
80. Tasdemir D, Kaiser M, Brun R, Yardley V, Schmidt TJ, Tosun F, *et al*. Antitrypanosomal and antileishmanial activities of flavonoids and their analogues: *in vitro, in vivo*, structure-activity relationship, and quantitative structure-activity relationship studies. Antimicrob Agents Chemother. 2006;50(4):1352-1364. DOI: 10.1128/aac.50.4.1352-1364.2006.